

# PHOTON VIOLATION SPECTROSCOPY

Eric Stanley Reiter

This is a March 2023 edit of my June 30, 2005 US patent application US-20050139776 A1.

## ABSTRACT

The method uses spontaneously emitted gamma-rays from a radioisotope source, typically cadmium-109 at 88 keV or cobalt-57 at 122 keV. Detectors employed are typically NaI(Tl) or HPGe. After a two-part gamma-ray split, detection pulses are windowed for the characteristic pulse amplitude and measured in coincidence. By using high resolution detectors and gamma-ray frequencies whereby the detector has a high photoelectric effect efficiency, coincidence rates are found to substantially exceed the chance rate, in defiance of quantum mechanics. This unquantum effect implies that photons are an illusion, and is explained by an extension of the long abandoned loading theory of Planck. In scattering gamma-rays in beam-split geometry, changes in response to magnetic fields, temperature, and crystal orientation become tools to measure properties of atomic bonds in the beam-splitter material. With detectors in tandem geometry where the first detector is both scatterer and absorber, tests reveal properties consistent with a classical gamma-ray model. The unquantum effect has also shown sensitivity to the crystalline state of the source material. Conventional gamma-ray spectroscopy shows no substantial response to these applied variables.

## BACKGROUND

The following thought experiment is important in the history of physics. In N Bohr's book, *Atomic Physics and Human Knowledge* (1958) pg. 50, he describes his 1927 discussions with Einstein and describes Einstein's two-part beam-splitter thought experiment:

"If a semi-reflecting mirror is placed in the way of a photon, leaving two possibilities for its direction of propagation, the photon would be recorded on one, and only one, of two photographic plates situated at great distances in the two directions in question, or else we may, by replacing the plates by mirrors, observe effects exhibiting an interference between the two reflected wave-trains."

This beam-splitter test is the principle of the photon. It is the first half of this quote that describes a particle property of light. The meaning of this thought experiment was clearly elaborated upon by Heisenberg in his book *Quantum Theory* (1930) pg. 39. Heisenberg concluded that a probability-amplitude wave undergoes an instantaneous "reduction of the wave packet" upon finding the photon in one part of the beam-splitter so as to eliminate finding the photon in the other part. De Broglie also discusses a version of Einstein's thought experiment in terms of a

generalized particle, not just photons, in *An Introduction to the Study of Wave Mechanics* (1930) pg. 142.

An early version of Einstein's beam-splitter test was performed by MP Givens, "An experimental study of the quantum nature of x-rays," *Philos. Mag.* 37 (1946) pgs. 335-346, whereby x-rays from a Coolidge tube were directed at a NaCl target. The x-rays were arranged to Bragg reflect and split into two beams toward Geiger-Mueller detectors. X-ray events detected in coincidence did not exceed the low rate expected by chance, consistent with the quantum mechanical prediction. They did not break chance.

In another beam-splitter test, visible light was tested to see if detector pulses in coincidences could defy chance, performed by E Brannen and HIS Ferguson in "The question of correlation between photons in coherent light rays" *Nature*, 4531 (1956) pg. 481. They used a filtered mercury arc line as a source, a beam-splitter, and two photomultiplier tubes (PMT) as detectors, and searched for coincidences from pulses from the PMTs. The coincidences detected did not break chance. These authors state "if such a correlation did exist it would call for a major revision of some fundamental concepts in quantum mechanics."

An experimental beam-splitter test designed to detect one  $h\nu$  released at a time was not

published until 1974 by JF Clauser in, "Experimental distinction between the quantum and classical field theoretic predictions for the photoelectric effect," *Phys. Rev. D*, 9 (1974) pgs. 853-860. Clauser used an elaborate scheme that delivered a gating pulse in a two-photon emission cascade, and used PMT detectors. His result was chance: a time-difference histogram ( $\Delta t$  plot) that was a featureless flat distribution, as expected by quantum mechanics. Recent writing by Clauser in *Coherence and Quantum Optics VIII*, ed. Bigelow (2003) pgs. 19-43 "Early history of Bell's theorem" reviews his beam-splitter test, showing he still maintained: "The experiment's results show that both quantum mechanics and quantum electrodynamics hold true, and photons do not split at a half silvered mirror."

A similar experiment to that of Clauser's was performed by P Grainger, G Roger, A Aspect, "A new light on single photon interferences," *Ann. N Y Acad. Sci.* 480 (1986) pgs. 98-107, and I quote them:

"... quantum mechanics predicts a perfect anticorrelation for photodetections on both sides of the beam-splitter, while any description involving classical fields would predict some amount of coincidences."

A review article featuring the work of Grainger et al, by AL Robinson appeared in *Science* 231 (1986) pg. 671, "Demonstrating single photon interference." In his opening statement I quote:

"One of the hallmarks of quantum mechanics is the wave-particle duality of matter at the atomic level. Sixty years of theory and experiment provide no reason to doubt the proposition despite the strange consequences that can follow."

This was an article about an experiment with light, yet it clearly implied a wave-particle duality for matter as well as light. All modern physics agreed.

There are patents, such as 06,188,768 issued to IBM on Feb. 13, 2001, that depend on the quantum mechanical interpretation of these prior art beam-splitter experiments. I quote from this patent:

"This is possible because single photons cannot be split into smaller pieces (intercepted or diverted photons simply won't arrive at the

intended destination) ..." (parenthesis in original).

Obviously a great investment has been made by the industrial and scientific communities in the idea that light is photons, and that it is not possible to break chance in the beam-splitter test. I have found no evidence in the scientific literature of any measurement that violates quantum mechanics or the principle of the photon in any manner remotely similar to the method I have developed and describe in this disclosure. To my knowledge, there is no prior art in any method of measurement based upon the failure of quantum mechanics. Quantum mechanics has never before been shown to fail for light in such a convincing manner as I will show. The only prior art in support of my method is theoretical.

A classical alternative to quantization, as applied to light, was called the loading theory. The earliest works I could find on the loading theory are from what is known as Planck's second theory. The history of Max Planck's second theory is described in T Kuhn's *Black-Body theory and the Quantum Discontinuity 1894-1912* (1978) pg. 235. In Planck's "Eine neue Strahlungshypothese" of 1911, an article found in a collection of Planck's works *Physikalische Abhandlungen und Vorträge* (1958) volume 2, he introduces a quantity of energy  $\epsilon$  that can have any value between 0 and  $h\nu$ , where  $h$  is Planck's constant and  $\nu$  is electromagnetic frequency. Planck used this  $\epsilon$  in his derivation of the black body distribution. Planck modeled, that light absorbers could have any initial energy up to a threshold of energy  $h\nu$ . Later in his book *The Theory of Heat Radiation*, a Dover translation of his 1913 "*Warmestrahlung*," Planck clarifies his model by stating on pg. 153

"Now, since in the law of absorption just assumed the hypothesis of quanta has as yet found no room, it follows that it must come into play in some way or other in the emission of the oscillator, and this is provided for by the hypothesis of the emission of quanta."

Planck's quanta were only at the point of emission. Planck then explains

"...an oscillator will or will not emit at an instant when its energy has reached an integral multiple of  $\epsilon$ ."

This is Planck's threshold concept. Kuhn describes how Planck had later abandoned this theory of continuous absorption and explosive emission.

The only other work I could find on the loading theory was by P Debye and A Sommerfeld in "Theorie des lichtelektrischen Effektes vom Standpunkt des Wirkungsquantums" *Ann. d. Physik* 41 (1913) pg. 78, where they calculate how an electron would be driven by a light field until the electron escaped. The loading theory was mentioned in Compton and Allison's book *X-Rays in Theory and Experiment* (1935) pg. 47, and Millikan's book *Electrons (+ and -)* (1937) pg. 253.

We were warned against light quanta by many greats in physics. I quote my translation of HA Lorentz from "Die Hypothese der Lichtquanten" *Physik. Zeitschrift*, 11 (1910) pg. 349:

"Light quanta which move concentrated in a small space and always remain undivided are completely out of the question."

## INTRODUCTION

This invention relates to transcending the following general assumption in physics: an absorption event that releases a quantity of energy is due to a particle of that same quantity of energy landing on the absorber. To understand this work, a conceptual shift is required in terms of thresholds instead of quanta.

The practical application of this new physics is measurement in material science. In physics, the new method requires replacing a quantum mechanical probability wave with a physical wave. The method is a beam-split coincidence test using gamma-rays. In all previous beam-splitter tests, there has been no evidence contradicting the idea that a quantum of energy goes only one way or the other at a beam-splitter. Prior beam-split coincidence tests delivered chance. Here, to defy chance required using: gamma-rays, certain radioisotope sources, and high resolution detectors. This implies that a single spontaneous decay will emit a gamma-ray that radiates classically, and that an energy less than the originally emitted  $h\nu$  can gamma-trigger two detection events in coincidence.

I call my violation of quantum mechanics the *unquantum* effect.

In a practical applications one measures the ratio exceeding chance (the unquantum effect). Then comparisons are made to see how the unquantum effect changes under different conditions.

After seeing that an unquantum effect is present, the pulse-height window of the second detector can be widened to see spectra. These coincidence-gated pulse amplitude spectra can reveal ratios of Rayleigh scattering to Compton scattering. Such a ratio can determine if the gamma-ray interacted with a stiff or flexible charge-wave in a material under study.

If the gamma-ray can split into two (so to speak), it can split into three or four, and this is another interesting mode of operation. Several such modes have been tested. The variety of geometries, detectors, modes of detection, conditions imposed on the scatterer, and chemical states of the source makes for a rich spectroscopy. This spectroscopy can serve to probe atomic bonds.

## THEORETICAL BACKGROUND

It is important explain history and theory leading to my discovery. Without this background it is easy to falsely assume that my findings do not make sense in the context of modern physics. To show that the physics behind this invention is reasonable I will derive equations for the Compton and photoelectric effects without resort to energy quantization, and I will reveal misleading ideas found in most physics textbooks.

Schrödinger first described a wave-oriented understanding of the Compton effect, and also a wave derivation is in Compton and Allison's book, *X-Rays in Theory and Experiment* (1935). The algebra is the same as my derivation below, except that my physics model removes an important difficulty. Compton describes x-rays being Bragg reflected by a diffraction grating made of electron-matter-waves composed of standing waves of Schrodinger's  $\Psi$  separated by  $\frac{1}{2}$  deBroglie wavelengths. In the light-charge interaction the Bragg grating recoils causing a Doppler shift in the

Bragg reflected electromagnetic wavelength. In that Bragg reflection model, they use a stationary frame component of the standing wave. However, there is no experimental justification toward modeling a stationary frame  $\Psi$  of comparable amplitude to the recoiling  $\Psi$  component, that together would generate a workable standing wave. Such a laboratory frame charge-wave can be going in any direction such that its addition to the forward component charge-wave would create only a very weak plane of standing wave to reflect light. My model postulates, with experimental justification, that there is a fundamental envelope property of charge-waves, with wavelength

$$\lambda_g = (h/m_e)/v_g, \quad Eq. (1)$$

where  $\lambda_g$  is the wavelength of a group, a beat of  $\Psi$ , and  $v_g$  is the velocity of the charge-beats. Eq. (1) looks like the deBroglie equation but differs in the meaning of its terms. Numerically  $m_e$  is the same as the mass of the electron, but I ask that it be viewed as the resistance to acceleration of an envelope of charge-wave.  $h/m_e$  was written together for a reason you will see later. De Broglie's equation uses the wavelength of the  $\Psi$  wave, whereas in Eq. (1) I use the length of an envelope of the  $\Psi$  wave. In GP Thomson's book, *The Wave Mechanics of Free Electrons* (1930) pg. 127, he states:

"...observing the heterodyne waves instead of the original wave train. It does not, however, affect questions of wave-length or of the motion of the original particles."

Here the expression for the motion of the particles may be understood in the usual quantum mechanical sense as detection events. GP Thomson considered the envelope interpretation, that I use, and found it consistent with his charge diffraction experiments. However, in exploring many works, no one used a group-length, the length of a beat, in the wave-length equation. De Broglie's version used a full wave length of  $\Psi$ .

My use of wave-beats that hold themselves together affords a recoil response to incident radiation. This removes the stationary frame component Compton employed to create standing waves for his wave oriented derivation. To be

accelerated by an incident x-ray I model charge to be free or in a loose bond. Bragg reflection from standing charge-beats in atomic bonds also explains Rayleigh scattering, where there is no wavelength shift. We use the Bragg diffraction equation  $\lambda_L = 2d \sin(\phi/2)$ . Here  $\lambda_L$  is the wavelength of light and  $\lambda_g$  is the wavelength of a charge-beat. Solve for  $d$  in the Bragg Eq. and insert in Eq. (1), realizing the spacing of the diffraction grating  $d$  is the length of charge beats:  $\lambda_g = d = \lambda_L/2\sin(\phi/2) = h/(m_e v_g)$ . Solve for  $v_g$  and insert it in the Doppler shift equation  $\Delta\lambda_L/\lambda_L = (v_g/c)\sin(\phi/2)$ . Simplify using  $\sin^2\theta = (1 - \cos 2\theta)/2$  to yield  $\Delta\lambda_L = (h/m_e c)(1 - \cos\phi)$ , the Compton effect equation. The Compton effect is popularly taught using conservation of particle momentum to convey that this effect is strong evidence for particles. One might say the  $h$  and  $m_e$  terms imply particles. However, the equation contains their ratio  $h/m_e = Q_{h/m}$ . This ratio, or similar ratios of  $h$ ,  $e$ , and  $m$ , always accompany experiments related to wave effects of charge. That ratio allows action and mass to individually become less dense, to thin-out, while the ratio itself is preserved. We do not measure  $h$  or  $m_e$  in this experiment; only the ratio  $Q_{h/m}$ . So the message of the experiment should be written  $\Delta\lambda_L = (Q_{h/m}/c)(1 - \cos\phi)$ . To summarize, nature expresses particle-like properties when the wave reaches the  $h$  threshold value, and expresses the wave properties by keeping this  $Q$  ratio constant as the wave spreads out. If we go back to Planck's 1911 paper and use action instead of energy, as the variable that reaches a threshold, the results of his derivation will be the same.

Now for the photoelectric effect. The overwhelmingly accepted derivation for its equation called for an inexplicable quantization of the electromagnetic field. The photon model of Einstein "On a heuristic point of view concerning the production and transformation of light" (title translated) *Ann. d. Phys.* 17 (1905) pg. 132, gained popularity because the equation fits experiment. However, if a model generates an equation that fits experiment, it does not eliminate the possibility that another model can generate the same equation. Our textbooks always use particle models to derive

the photoelectric and Compton effects, and then use experimental confirmation of the equation to attempt to prove that the effect requires their particle model. Sommerfeld in his book *Wave Mechanics* (1930) pg. 178 describes Einstein's photoelectric effect law as

“not actually derived.”

To my knowledge, no one has linked the photoelectric equation to the deBroglie equation in any derivation, as I do below.

To show that a particle model is not required, my derivation uses the charge-wave beat model. This model is also similar to a description found in Schrödinger's famous paper “Quantization as a problem of proper values,” *Annalen der Physik* (4), vol. 79 (1926). He uses the word 'beat' also. The Balmer equation of the hydrogen spectrum reveals that the light frequency  $\nu_L$  is the result of the difference between two frequency terms of  $\nu_\psi$ . In its simplest form the Balmer equation can be expressed as:

$$\nu_L = \nu_{\psi_2} - \nu_{\psi_1} \quad Eq. (2)$$

From these difference-frequencies, plus Schrödinger's suggestion that light interacts with the beats, I use a trigonometric identity:

$$\begin{aligned} \Psi_{\text{total}} &= \Psi_1 + \Psi_2 = \cos 2\pi[(x/\lambda_{\psi_1}) - \nu_{\psi_1}t] + \\ &\cos 2\pi[(x/\lambda_{\psi_2}) - \nu_{\psi_2}t] = \\ &2\cos 2\pi[(x/\lambda_{\psi_a}) - \nu_{\psi_a}t] \cos 2\pi[\Delta(1/\lambda_\psi)x/2 - \\ &\Delta\nu_\psi t/2] \end{aligned}$$

where the second term in the right hand side is a modulator wave at frequency  $\Delta\nu_\psi$  that shapes the first term, an inner average  $\Psi_a$  wave. From this model, we count two beats (groups) of  $\Psi$  per modulator wave and realize the modulator wave frequency  $\Delta\nu_\psi$  equals the light frequency:  $\Delta\nu_\psi = \nu_L$ . This was all done just to show that the frequency of two beats of charge fit the frequency of a light wave. Light fits the modulator term in the trigonometric identity. In terms of frequency:

$$2\nu_L = \nu_g \quad Eq. (3)$$

For anything periodic, including beats, velocity equals frequency times wavelength. Substitute *Eq. (2)* and *Eq. (3)* into  $\nu_g = \nu_g \lambda_g$  to get:

$$m_e \nu_g^2 / 2 = h \nu_L, \quad Eq. (4)$$

the equation for the photoelectric effect. Adding a term for escaping a potential is an obvious refinement.

The photoelectric *experiment* does not deliver all terms expressed in *Eq. (4)*. We may measure frequency and velocity, or equivalently we may measure frequency and electrical potential, but we borrow  $e$  or  $m_e$  from different experiments. The message of the photoelectric effect experiment, independent of other experiments, must be written:

$$\nu_g^2 / 2 = Q_{h/m} \nu_L, \quad Eq. (5)$$

where  $Q_{h/m} = h/m_e$ . When the equation is in terms of electron volts we use  $Q_{h/e}$ . When the wave spreads in free space we only read the various ratios of action, mass, and charge in our experiments. In free space the  $Q$  ratios are the constants, and  $h$ ,  $m_e$ , and  $e$  are maximums that we have individually deciphered only through experiments using condensed matter. Similarly *Eq. (1)* should be written  $\lambda_g = Q_{h/m}/\nu_g$ , to account for the spreading wave and a mechanism for the loading effect. The  $Q$  ratios I mentioned are  $Q_{h/m} = h/m_e$ ,  $Q_{e/m} = e/m_e$ , and  $Q_{e/h} = e/h$ . In wave experiments containing ratios of these terms, we only measure the  $Q$  ratios. Experiments containing higher powers of our constants describe systems that are more particle-like.

My unquantum effect would not be possible if electromagnetic energy was quantized. My theory led me to predict the experimental evidence displayed here. The threshold concept explains the spreading wave by allowing a thinning-out of charge, mass, and action, while keeping them in proportion. A threshold reached at absorption explains our particle-like detection clicks. In contrast, quantized absorption requires a non-local wave-function collapse.

In developing the concept of a wave associated with particles, de Broglie derived his famous relation

$$h = m_p \nu_p \lambda_p, \quad Eq. (6)$$

where  $m_p$  is total relativistic particle mass,  $v_p$  is particle velocity, and  $\lambda_\psi$  is phase wavelength of a matter-wave function  $\Psi$ . After Eq. (6) was endorsed by Einstein, used by Schrödinger, and shown to be consistent with electron diffraction, the equation was routinely used. The mixture of wave and particle terms in Eq. (6) inescapably preserves wave-particle duality in quantum mechanics. Intimately linked to the derivation of Eq. (6), de Broglie assumed a matter frequency  $\nu_\psi$  using the relations:

$$\epsilon_p = m_p c^2 = h \nu_\psi, \quad \text{Eq. (7)}$$

where  $\epsilon_p$  is mass-equivalent energy plus kinetic energy of a particle. Notice that this association of  $h$  with a matter-frequency  $\nu_\psi$  is very different from the way  $h$  is used in any experiment except for the case of pair production/annihilation. We never measure this matter frequency. When  $h$  enters analysis of black body, photoelectric, Compton effect, and other experiments,  $h$  relates to kinetic energy or momentum. The link between Planck's constant and mass-equivalent energy has only entered our conceptual framework through this great leap of faith made at Eq. (7). With this overview, our experiments are telling us that  $h$  is really about kinetic energy, not mass-equivalent energy. From deBroglie's early books, such as *An Introduction to the Study of Wave Mechanics* (1930), one can see that Eq. (7) came from a symmetry argument using the dualistic model of the photoelectric effect as a starting point. If one uses Eqs. (6) and (7), and puts  $\nu_\psi$  and  $\lambda_\psi$  into  $v_\psi = \nu_\psi \lambda_\psi$ , it leads to

$$v_p v_\psi = c^2 \quad \text{Eq. (8),}$$

where  $v_\psi$  is phase velocity of a probabilistic  $\Psi$  matter wave. Alternatively, one can use dimensional analysis on the Lorentz transformation of time to extract Eq. (8) and derive Eq. (6). For arbitrarily slow particles, Eq. (8) implies arbitrarily fast  $\Psi$  velocities. A stationary particle implying some infinite velocity should have warned physicists that there was something wrong with the derivation of the de Broglie equation and quantum

mechanics. Instead Eq. (8) is often used in our modern textbooks and literature to show  $\Psi$  is not physical. See for example M Born *Atomic Physics* (1935) pg. 89. If we assume any physical sense for  $\Psi$  that is not just some mathematical convenience, the specific forms of equations (7 and 8), and even (6) must be abandoned.

Returning to the Compton effect, a famous test was the experiment of Bothe & Geiger, where an x-ray beam interacting with hydrogen is measured for coincident electron and x-ray photoelectron events. The experiment was intended to test if a wave model developed by Bohr, Kramers and Slater could serve as an alternative to quantum mechanics. The theory of Bohr et al was about spherical x-ray wave-fronts to induce electron events on a statistical basis. Momentum was only conserved on the average and not for each electron event. The statistical nature of the theory predicted that electron events would not synchronize to photoelectron events. The experiment by Bothe and Geiger reported that the rate of synchronized events happened more often than chance, but not as often as would be expected from a purely particle model either. The partial particle-like results of the Bothe-Geiger experiment was enough for Bohr et al to abandon their model. Afterwards, all writings took on an even stronger particle-bias. From my examining the original work in German, the assessment by Bothe and Geiger was only reservedly in favor of the particle model of Compton since their data showed that only sometimes the events are synchronized, and mostly they are not. From the Bothe-Geiger experiment, approximately only one in 2000 events were simultaneous before calculating detector inefficiency, and the corrected rate is 1/11. If particles were the cause, this rate would be much higher. Many experiments have been done to measure simultaneity in the Compton effect. Except for the 1936 analysis of Shankland, "An apparent failure of the photon theory of scattering," *Physical Review* 49 (1936) pg. 8, all works thereafter, as evidenced by a review article by Bernstein and Mann, "Summary of recent measurements of the Compton effect," *American Journal of Physics* 24 (1956) pg. 445, missed the point, and concentrated instead on how many nanoseconds within which a pair of events are

simultaneous. My research found no report later than 1936 giving any number for the degree of simultaneity between electron and x-ray events, other than the shortest time between them. Much commentary on this experiment falsely reports a one-to-one correspondence between “photon” and electron events. A similar situation persists in how the scientific community misrepresents the message of the data of the Compton-Simon experiment.

Data from Bothe, Geiger, "Über das Wasen des Comptoneffekts," *Z. Phys.* 26 (1924) pg. 44, fits my wave model. The electron detection rate was  $6 e/s = I_a$ , but this detector was 200 times more efficient than the x-ray detector. The window of simultaneity  $\tau$  was 1 ms. Using the equation for shot noise  $I_n = (2I_a e/\tau)^{1/2}$ ,

$$I_n = [(2)(6 e/s) / (10^{-3} e/s)]^{1/2} = 115 e/s. \quad Eq.(9)$$

This gives  $I_a/I_n = 6/115$ , 20 times more noise current than the average current. Accounting for the factor of 200 detector inefficiency gives 4000 events/coincidence. Since each detector picked up only half a radiated sphere, divide by two to get 2000 events/coincidence, which matches data from the experiment. Shot noise shows that the observed simultaneity is what would be expected from this type of beating spreading wave.

The issue of simultaneity in the Compton effect is a good example of how a particle-biased mindset has influenced the transmission of information from experiment to our textbooks. For example, in a paper by Compton and Simon, "Directed quanta of scattered x-rays," *Physical Review* 26 (1925) pg. 289, in their abstract they write:

"It has been shown by cloud expansion experiments previously described, that for each recoil electron produced, an average of one quantum of x-ray energy is scattered by the air in the chamber."

Not true. Amazingly, even Compton in his *Scientific American* article, "What things are made of" Feb. 1929, p. 110, and most authors afterwards, did not accurately relay the message of this experiment to us. They conveyed that momentum is conserved in “each” detector event, like macroscopic balls. A billiard-like model is unfounded because the average nature of the effect

was demonstrated by the high rate of non-simultaneous events reported in both the Compton-Simon and the Bothe-Geiger experiments.

Now to the black body equation. I performed a derivation of Planck’s black body distribution using charge beats instead of standing waves of light. There are many ways to do the derivation, and most of Planck's used Hertzian oscillators, not light. See Planck's 1906 *Theorie Der Warmestrahlung*. Most of our textbooks use a standing-wave-of-light model to derive the Planck distribution. The fact that cosmic microwave background radiation obeys the black body distribution makes it clear that standing waves of light cannot possibly be the underlying mechanism. There are no mirrors making the standing waves. Such a thing would require the whole universe to act as an absurd perfect laser cavity. Further analyses of mine address the folly of assuming charge must be quantized in free space, based upon Millikan’s oil-drop observations. See my essay “An Understanding of the Particle-like Property of Light and Charge.”

A very popular and misleading argument concerns the response-time in the photoelectric effect. A typical case is in the popular text *Fundamentals of Physics second edition extended* by Halliday and Resnick (H&R). Given a light source and the size of the atom one can calculate the time an atom should take to accumulate enough energy to eject an electron. The student calculates some number of minutes, and then the text cites an experimental response time on the order of a nanosecond. The experiment is by Lawrence and Beams (L&B), "The element of time in the photoelectric effect," *Physical Review* 32 (1928) pg. 478. The light flux L&B used was not stated. Our textbooks explain that

“no time lag has ever been detected.”

From L&B’s data, their minimum response time was about 3 nanoseconds, but they report times up to 70 ns. There are several problems. Since L&B did not report incident light flux, one cannot compare their response time to a time based on that textbook example. The other problem is that by H&R stating “no time lag has ever been detected,” it falsely represents the results of the experiment; the experiment *did* report an *average* time lag. An average time lag is consistent with

the idea of a pre-loaded state, but this idea was not given a chance when they denied any form of time lag. Consideration of the pre-loaded state seems to have been banished from our literature ever since Millikan considered it in *Electrons (+ and -)*. Since then every book or article I could find is written with the assumption that an accumulation starts from zero when the light is first applied. If a pre-loaded state is allowed to exist, a classical calculation can use the average response time, and energy conservation to calculate a reasonable incident energy flux. Authors should write: no *minimum* time lag has ever been detected. By stating that “no time lag” exists when in fact an *average* time lag does exist, textbook authors have effectively propagandized photons. Another problem is to assume the size of the absorber is the size of the atom. Antennae theory says the size can be much larger.

With this above outline of long standing conceptual problems in quantum mechanics, errors perpetuated in our textbooks, and seeing that the photoelectric effect and the Compton effect can be derived with waves, my evidence for an unquantum effect disclosed here stands to reason.

## COMPARISON TO PRIOR ART

In a 1946 beam-splitter test by Givens, a Coolidge x-ray tube was used. A tube will always generate many  $h\nu$  of overlapping Gaussian pulses. Such pulses could easily average out to a smooth energy flux, greatly lowering the chances that a single  $h\nu$  would reveal a loading theory. Wide-band emitters and detectors would further obscure a classical response. Givens used Geiger-Mueller counters which do not deliver a pulse proportional to electromagnetic frequency. Furthermore, no pulse amplitude analysis or discriminator levels were reported. My method takes advantage of modern detectors that delivers pulse amplitude proportional to electromagnetic frequency. Both time and energy needs to be accounted for in this argument. Furthermore, a wide range of frequencies present will quench any possibility of reading coincident detector clicks, if a tuned microscopic absorber were to reach a threshold. Furthermore, my method takes advantage of pulse-like single  $h\nu$  emission from radioactive decay.

Also, I use a low count rate to prevent overlapping classical pulses from smoothing the pulse-like spatial and temporal quality of the energy flux. The test by Givens was inadequate to make a quantum/classical distinction.

Clauser, and all others attempting this beam-splitter test made a crucial error concerning the PMT. Even if the source of light is monochromatic, a PMT will generate a wide distribution of pulse amplitudes. A typical pulse amplitude distribution from a PMT is about as wide as the amplitude at the peak of this distribution. In my extensive search, no test of Einstein’s beam-splitter thought experiment specifies their pulse amplitude discriminator settings. However, experimenters always use discriminators to eliminate the small and frequent pulses, usually attributed to noise. By eliminating the smaller pulses in the pulse amplitude distribution, it greatly lowers the possibility of detecting coincidences allowed for by the loading theory. Alternatively, if such discriminators are not used, it is not fair with respect to the photon model. Essentially, this type of experiment cannot make a fair classical/quantum distinction using optical light and PMTs because the PMT delivers too wide a distribution of pulse amplitudes in response to monochromatic light.

Another important oversight in Clauser’s experiment is that he describes using a polarizing beam-splitter. Data from CA Kocher and ED Commins, “Polarization correlation of photons emitted in an atomic cascade,” *Physical Review Letters* 18 (1967) pgs. 575-577, show that single  $h\nu$  emissions from atoms are polarized. A randomly polarized pulse of light will be unequally split by a polarizing beam-splitter, thereby lowering the opportunity for coincidences. This would unfairly eliminate the classical alternative that the experiment was supposed to distinguish from quantum mechanics. This flaw, plus false assumptions concerning the PMT, voids Clauser’s result.

In my research of over a hundred articles directly referencing Clauser’s 1974 paper, including Grainger et al’s 1986 rework, and Clauser’s own recent articles, these important technical oversights concerning the detector

resolution and polarized beam-splitter have remained uncorrected.

## NON-OBVIOUSNESS

One would think that it would be obvious to try the beam-splitter test with gamma-rays to show how to defy quantum mechanics. Einstein's beam-splitter thought experiment has been well known since 1927. However, the way to manage an energy that obeys  $E = hv$ , and split it in a manner that breaks chance has not previously been accomplished. No one has previously considered using gamma-rays, the most particle-like light, to show that light is not particles. Everyone took it as a fact that gamma-rays are photons. For example, a well respected book edited by K Siegbahn *Alpha Beta and Gamma-ray Spectroscopy* (1962) contains the article by CM Davison "Interaction of  $\gamma$ -radiation with matter" with the opening line

"The interaction of  $\gamma$ -radiation with matter is characterized by the fact that each  $\gamma$ -ray photon is removed individually from the incident beam in a single event."

If gamma-rays were photons, my experiments would not break chance.

To visualize how classical light could break chance in the beam-splitter test requires understanding: (1) how electromagnetic emission could be pulse-like, and (2) how a preloaded state could create the illusion that a particle hit there. It requires understanding how an electromagnetic pulse of initial energy  $hv$  could split as a wave and cause coincidences. It requires understanding how a set of oscillators at random levels of a partially loaded states could be fed energy in a continuous fashion, and how the time to reach a threshold of fullness in a loading mechanism would be random. To break chance, it requires understanding how a classical electromagnetic pulse with energy less than or equal to  $hv$  may be partially absorbed by separate resonant absorbing centers, and then trigger a coincident loading-to-threshold  $hv$  at these absorbing centers at rates surpassing chance. To solve this difficult puzzle required all the theory I outlined in the THEORETICAL BACKGROUND section.

From my theoretical work and historical analysis up to year 2000, I knew that a source

emitting strong individual  $hv$  bursts was needed; with that knowledge it makes sense to consider gamma-rays. My early attempts to search for the unquantum effect with the simple idea of using gamma-rays were failures. My early attempts with radioisotopes Na22 and Cs137 only gave chance. The unquantum effect only showed itself after I realized the related properties of source and detector. There were many obstacles to overcome:

- (1) In choosing a gamma source, there must not be other gamma, emitted simultaneously with the same gamma under study. There are few long lived radioisotope sources that emit one characteristic gamma-ray.
- (2) There are very few gamma sources available whereby a high photoelectric effect efficiency resides in a high resolution detector.
- (3) An initially unrecognized contaminant in Cd109 caused a peak at exactly 3 times its 88 keV photopeak and emitted other frequencies that obscured an expected 2 x 88 keV anomalous sum-peak.
- (4) Our highest resolution detectors have lower photoelectric efficiency, so in a situation that a scientist would normally think they see better, they see worse.
- (5) A fluorescence from lead fell at nearly the same keV as the 88 keV of Cd109, which could confuse interpretation.
- (6) I had no support from any physicist because they all knew gamma-rays acted like particles.

## BRIEF DESCRIPTION OF THE FIGURES

Fig. 1 shows the pulse amplitude response of a typical photomultiplier tube responding to visible light.

Fig. 2 shows annotated pulse amplitude spectra, using Cd109, Co57, and a high resolution germanium type detector.

Fig. 3 shows annotated pulse amplitude spectra, using Cd109, Co57, and a sodium iodide type detector to study sum-peak details.

Fig. 4 shows a preferred embodiment of this invention with one detector in front of another in tandem geometry.

Fig. 5 shows detail of detectors used for selected tandem geometry experiments.

Fig. 6 shows a section of screen capture from my oscilloscope of a coincidence time plot ( $\Delta t$  plot), using Cd109, and detectors described by Fig. 5 in tandem geometry.

Fig. 7 shows coincidence time plots, using Cd109, Cs137, a signal generator, and sodium iodide detectors in tandem geometry.

Fig. 8 shows coincidence time plots, using Cs137, and sodium iodide detectors in tandem geometry to study effects of distance and attenuation.

Fig. 9 shows coincidence time plots, using Co57, and sodium iodide detectors in tandem geometry to study effects of distance.

Fig. 10 shows a coincidence-gated pulse amplitude plot (histogram), using Cd109, a high resolution germanium detector, and a sodium iodide detector in tandem geometry. A singles spectrum of Cd109 is also shown.

Fig. 11A shows a section of screen capture from my oscilloscope of coincidence time plots, using three preparations of Cd109 in different crystalline states, and sodium iodide detectors in tandem geometry to study effects due to chemical state of the source.

Fig. 11B shows a section of screen capture from my oscilloscope of coincidence-gated pulse amplitude plots, using the same three preparations of Cd109 used in Fig. 11A, and sodium iodide detectors in tandem geometry to study effects due to chemical state of the source.

Fig. 12 shows a preferred embodiment of this invention in beam-splitter geometry equipped to adjust the angular orientation of a detector and the angular orientation of a material scatterer under study.

Fig. 13 shows coincidence time plots, using Cd109, and two sodium iodide detectors in beam-splitter geometry to study a silicon material scatterer at two angular orientations.

Figs. 14A and 14B show the relative size and orientation of two high resolution germanium detectors, source, and magnet assembly used in the tests of Figs. 15 and 16.

Fig. 15 shows coincidence-gated pulse amplitude plots, using Cd109, and two high

resolution germanium detectors in beam-splitter geometry to study a ferromagnetic scatterer in different magnetic fields.

Fig. 16 shows a section of screen capture from my oscilloscope of coincidence-gated pulse amplitude plots, using Cd109, and two high resolution germanium detectors in beam-splitter geometry to study a diamagnetic scatterer in different magnetic fields.

Fig. 17 shows the beam-splitter geometry relating to plots in Figs. 18 and 19.

Fig. 18 shows a section of screen capture from my oscilloscope of coincidence-gated pulse amplitude plots, using Cd109, and two high resolution germanium detectors in beam-splitter geometry to study an aluminum scatterer at different temperatures.

Fig. 19 shows a section of screen capture from my oscilloscope of coincidence time plots, using a salt state Cd109, a metallic state Cd109, and two sodium iodide detectors in beam-splitter geometry to study the difference, from the state of matter of two sources, upon a germanium scatterer.

Fig. 20 shows annotated pulse amplitude spectra, using a sodium iodide detector to study the same two sources used in the test of Fig. 19.

## DETAILED DESCRIPTION

### INTRODUCTION

My earliest successful evidence of the unquantum effect dates from August 8, 2001, with scores of experimental variations and upgrades performed since then. The unquantum effect is enhanced when using a detector with substantial pulse amplitude resolution for the radiation being measured. This implies: (1) the pulse amplitude is proportional to the electromagnetic frequency of the incident radiation, and (2) the distribution of pulse amplitudes in response to a given frequency of incident radiation is narrower than the mean pulse amplitude. Historically, experiments with the DuMond curved crystal spectrometer design of 1927 have confirmed the relationship between detector pulse amplitude and electromagnetic frequency. As mentioned in the COMPARISON TO PRIOR ART section, a photomultiplier tube used

with visible light does not deliver a good enough pulse amplitude resolution. Fig. 1 shows a typical pulse amplitude distribution **AA** of a PMT from a Phillips Photonics data book, *Photomultiplier tubes principles and applications*, (1994) pg. 2-8. I annotated this graphic. This distribution graph was similar to my own test with a red laser and a PMT. Fig. 1 graphs the pulse amplitude **18** versus counts **19**, with the peak of the distribution at pulse amplitude  $E_{\text{mean}}$  **20**, and the full width of the distribution  $\Delta E_{\text{window}}$  **21**. The boundaries of  $\Delta E_{\text{window}}$  **21** are typical positions for discriminator settings, also known as a single channel analyzer (SCA) window. Span  $\Delta E_{\text{mean}}$  **22** of pulse amplitudes up to point  $E_{\text{mean}}$  **20** is about the same distance in this case as span  $\Delta E_{\text{window}}$  **21**. Here we see what a typical experiment using a PMT must work with. If the window was set so that  $\Delta E_{\text{window}} > \Delta E_{\text{mean}}$  in a beam-splitter test, events in coincidence would be recorded too easily and would overshadow coincidences triggered by a classical pulse in a loading scheme; it would not be fair to the loading model. On the other hand, if we were to assume a photon model and were to set the SCA window narrower so that  $\Delta E_{\text{window}} < \Delta E_{\text{mean}}$ , too many events that could have been triggered by a photon would have been eliminated from being detected in coincidence; it would not be fair to the photon model. In other words, a beam-splitter test cannot make a distinction between a probability wave and a classical wave using a detector/source combination unless  $\Delta E_{\text{window}} < \Delta E_{\text{mean}}$ . This is the importance of adequate pulse amplitude resolution. A PMT does not have adequate pulse amplitude resolution. The detector that I usually use is a NaI(Tl) scintillator coupled to a PMT. These detectors working above  $\sim 40$  keV satisfy this criteria and do have adequate pulse amplitude resolution. This is one reason why my method gives the opposite result compared to the result of prior tests. To my knowledge, no prior attempt at the beam-splitter test has used a detector with adequate pulse amplitude resolution, and neither have they bothered to report discriminator (SCA) levels.

Indeed, there is great confusion over the interpretation of what a PMT delivers. Physicists generally think, to their great error, that the pulse

amplitude delivered by a PMT is faithfully proportional to the frequency of incident light. As evidence I quote RP Feynman *QED* (1985) pg. 15:

“...clicks of uniform loudness are heard each time a photon of a given color hits plate A.”

A distribution of click loudness that is as wide as the mean loudness is not a click of uniform loudness. This quote also demonstrates the false assumption: a photon is a thing existing prior to the detection event.

There are two geometries described in my experiments: a beam-splitter geometry and a tandem geometry. In tandem geometry, with one detector in front of another, the first detector performs the function of both the beam-splitter and detector, and shows the effect more efficiently.

It is necessary to make clear that notation eV for electron volts, is used here only for convenience to the reader. eV is a photon energy concept. Where a conventional physicist would describe photon energy, I may describe frequency or detector pulse amplitude instead. If gamma-rays are not photons, we should talk of frequency instead of energy. In conventional physics  $h\nu$  is often used to describe a photon energy. Here  $h\nu$  is an energy proportional to frequency (a) in matter at a threshold, and (b) in an initially emitted burst of electromagnetic energy. Here a quantum is an  $h\nu$  of energy at an internal threshold, or at an

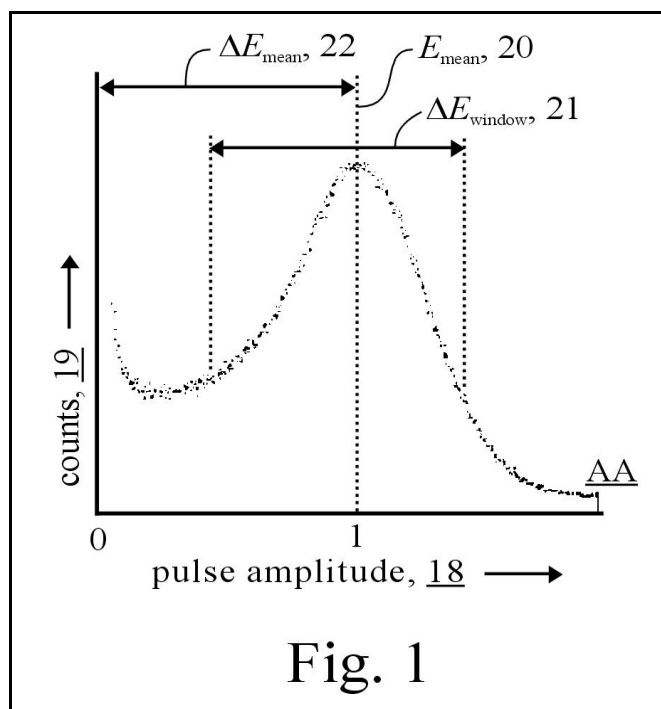


Fig. 1

initial release of light. Here we understand that after a quantum of light is released, the light does not remain quantized. An absorption or detection event is modeled as a resonant loading in an electronic oscillator, whereby the event occurs when a threshold is met within the electronic oscillator at energy  $h\nu$ . Quantum mechanics assumes in the photoelectric effect that an  $h\nu$  emitted from a source is the same  $h\nu$  absorbed as at a detector. Here we show that model's failure.

By comparing a chance coincidence rate  $R_c$  with an experimentally measured coincidence rate  $R_e$ , the experiment distinguishes classical from quantum mechanical models of light. If light really consisted of photons, or equivalently, if light always deposited itself in a photon's worth of energy, it would be a quantum mechanical wave function  $\Psi$  that would split, and the particle would only go one way or another at a beam splitter. After absorption the wave function would need to magically collapse. The consensus among all findable prior attempts of this beam-splitter test is that all coincident detection events from individually emitted quanta are attributed to chance. The evidence here demonstrate that  $E = h\nu$  applies to matter as a loading effect, and that  $E = h\nu$  cannot be due to a quantum mechanical property of light.

Two radiation sources have been found highly successful in measuring the unquantum effect: 88 keV gamma-rays from cadmium-109 (Cd109) and 122 keV gamma-rays from cobalt-57 (Co57). In both of these radioisotope sources, spontaneous nuclear decay is understood to occur in an electron capture process. Two detector types have been highly successful in detecting the unquantum effect: sodium iodide scintillator crystals doped with thallium, NaI(Tl), and high purity germanium (HPGe) detectors. Fig. 2 shows detector pulse amplitude spectra taken in my laboratory June 2003 using my HPGe detector, with graph axes of pulse amplitude **25** and logarithmic counts **26**. In most of my plots the vertical scale is offset to superimpose many plots upon the same horizontal scale. The detector is a CANBERRA GR1520 reverse electrode type. To minimize background radiation, all measurements reported in this disclosure were taken within a lead shield of my own fabrication: a cylinder 12 inches diameter,

15 inches long, with 2 to 3 inch walls of lead, lined with 2 mm of tin and 3 mm copper at its inside walls. In the range 56 to 324 keV, the average singles background rate in the shield was lowered to 1/31 of that read outside the shield.

Fig. 2 shows spectra of background **BA**, and Cd109 **BB**. The 88 keV **30** gamma-ray from Cd109 is a characteristic detector pulse amplitude. We know gamma-rays only through characteristics revealed in experiments. We interpret that an atom emits an initially directed classical pulse of electromagnetic energy at an electromagnetic frequency. Typical emitted bandwidths are known from other experiments to be much narrower than the bin widths of the spectra in my instruments. For this Cd109 characteristic gamma-ray emission, the detector responds with pulse amplitudes within range  $\Delta E$  **32**. From taking spectra like these on Fig. 2 one can determine the electromagnetic frequency of the gamma-ray and the rates  $h\nu$  are produced. However, we do not assume that a photon left the atom and landed at the detector.

It was discovered that Cd109 is often contaminated with Cd113m (m = metastable) that produces a 264 keV peak **34** and a continuum from 88 to 264 keV. By using a later-obtained source of Cd109 that was free of any detectable Cd113m and repeating a coincidence test, I confirmed that this contamination was not distorting coincidence counts in my experiments using two detectors. Cd113m did not create coincidences by Compton downshifting or any other mechanism. An x-ray **36** is also radiated by Cd109. A lower frequency from such an x-ray cannot lend to producing coincidences near the 88 keV section. Tests with a 2 mm aluminum filter to attenuate the x-ray showed no change in the unquantum effect. Spectrum **BC** of Co57 shows two gamma peaks, at 122 keV **46**, and 136 keV **48**. Published energy level diagrams devised from coincidence tests show there are separate pathways for these two frequencies. That means gamma-rays **46**, **48** occur independently. NaI(Tl) detectors cannot resolve these **46**, **48** peaks. Therefore a coincidence test using NaI(Tl) detectors windowed over both **46**, **48** gamma frequencies can be treated as if only one  $h\nu$  was emitted at a time. Other high

resolution detectors such as Cadmium Zinc Telluride may be considered.

There are two important absorption mechanisms in these detector materials: the photoelectric effect and the Compton effect. For the two isotopes that the unquantum effect easily reveals itself, it has been found that the photoelectric effect dominates. Most tests in this disclosure used a NaI(Tl)

scintillator coupled to a photomultiplier tube. In a sodium iodide scintillator detector reading an 88 keV gamma-ray emitted by Cd109, the photoelectric effect dominates over the Compton effect by a factor of 18. However using HPGe detectors this ratio is 4.6/1. This information is from graphs published by NIST generated from quantum mechanical calculations. This dominance of the photoelectric effect is similar with 122 keV from Co57 when comparing the two detector types. Also, at 88 keV, NaI(Tl) detectors have a peak in overall absorption efficiency. From studying this I predicted that the unquantum effect would be more easily seen with NaI(Tl) than HPGe detectors; this tested true from examining sum-peaks in single detectors and comparing them in both detector types.

The unquantum effect is also observable with a single detector, by carefully measuring the sum-peak that is produced by pile-up of pulses. The sum-peak is found at twice the pulse amplitude of the photo-peak gamma-ray. In this technique the detector material serves the purpose of detector, beam-splitter, and coincidence gate. The beam will split within the body of the detector. The summing of light-pulse energies within the scintillator performs the same function as the coincidence-gate electronics that are described for the preferred embodiments.

Fig. 3 shows logarithmic spectra of gamma-ray sources, detected by a 2 x 2 inch cylindrical BICRON brand NaI(Tl), recorded with a commercial multichannel analyzer, and with the sources placed

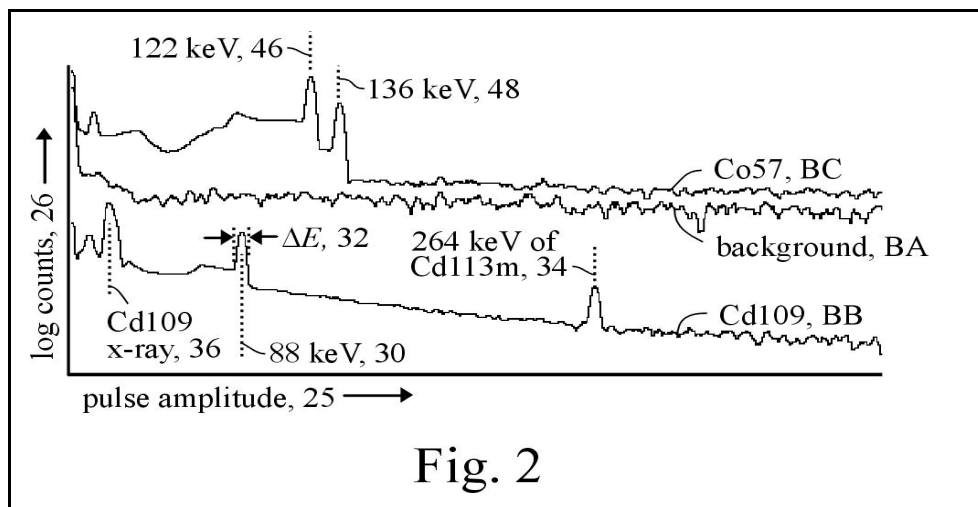


Fig. 2

at the top of the detector, taken October 2004. Plots are of: ~5 μCi of contaminated Cd109 due to Cd113m at plot CA, ~5 μCi of substantially pure Cd109 CB, ~5 μCi Co57 CC, and background CD. Here we see how the usual presence of Cd113 could easily hide an anomalously large sum-peak. A sum-peak is usually attributed to chance, and its amplitude is predicted by calculating the chance sum-peak rate as

$$R_{cp} = 2\tau R^2 \quad Eq. (10)$$

where  $\tau$  is the time span of each pulse that piles up, and  $R$  is the rate at the peak of the distribution that piles up to cause this sum effect. There is some controversy in the literature over the accuracy of this equation and how to choose the value of  $\tau$ . I have circumvented this problem by doing an experiment with Cs137 under conditions that display no appreciable unquantum effect, and used Eq. (12) to calculate  $\tau = 1.16 \times 10^{-6}$  sec. The shape is conserved with different amplitudes, so this time constant is also conserved.

The bin with the highest rate at 88 keV 58 in pure Cd109 gave  $R = 74.3/s$ . From Eq. (10),  $R_{cp} = 0.0064/s$ . For the experimentally measured sum-peak rate,  $R_e$ , an average was taken in the marked section 60 surrounding  $2 \times 88$  keV, and an average of the background at this spectral section was subtracted, giving  $R_e = 0.064/s$ . The ratio of (measured sum-peak rate)/(chance sum-peak rate) gives the degree that chance is exceeded, and calculates to:  $R_e/R_{cp} = 10 \times$  chance.

Similarly for Co57, examining section **62** at 2 x 122 keV, the singles rate at 122 keV **63**, and  $\tau$  gave  $R_e = 2(1.16 \mu\text{s})(67.8/\text{s})^2 = 10.7 \times 10^{-3}$ ;  $R_e/R_{cp} = 0.0107/0.00196 \approx 5.5 \times$  chance. This roughly tracks the idea that the effect is due to photoelectric dominance, which is less at 122 keV. These enormous spectral components will not vanish to chance with an alternative kind of chance calculation. I have only been observed them in Cd109 and Co57. These sum-peak areas are shaped more like plateaus than peaks. In my research I explained this shape by writing a simulation program that input the whole spectral region of characteristic gamma and Compton shifted components. A typical SCA window used in my experiments is shown at  $\Delta E$  **64** of Fig. 3.

A more convincing test is to use two detectors one in front of the other, in tandem. In this technique the material of the first detector serves the function of both detector and beam-splitter. The components and most techniques described here on, are well known in the nuclear measurement industry. What is not known is to how to set aside the particle model.

### PREFERRED EMBODIMENT USING TANDEM GEOMETRY

The apparatus of Fig. 4 is useful for demonstrating and researching the unquantum effect under various conditions, distances, and mixtures of source. The entire apparatus should be in a box lined with at least 2 mm of sheet tin, not shown. This was tested to be adequate, but the experiments in this disclosure were all done in my lead shield. In most tests the unquantum effect is clearly apparent without the shield, but by lowering background radiation the shield gives better results. A Cd109 radiation source **68** of at least 1  $\mu\text{Ci}$  activity, in holder **70** is mounted in tin collimator **72**. Higher activities than 10  $\mu\text{Ci}$  are not typically needed in these tests, and such low level sources are available without licensing restrictions. The most versatile source holder **70** is a microcentrifuge tube wherein the radioisotope may be most conveniently

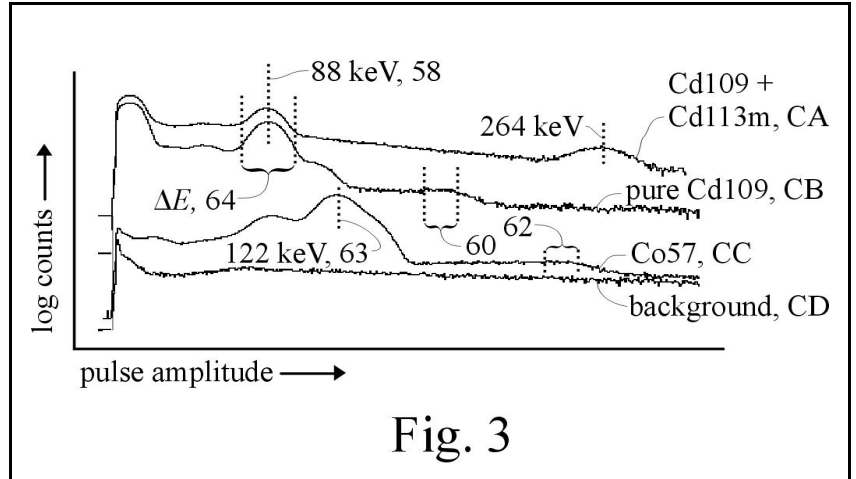


Fig. 3

prepared. These radioisotopes are available in solution and with mild heat its solid can be condensed. The detection hardware is best described as two channels. Each channel has a detector, preamplifier, shaping amplifier, and SCA circuit. Collimator **72** serves to define cone **74** of gamma-rays aimed toward channel 1 scintillator **76**. Collimator **72** is mounted on a linear translation stage **78** that can adjust the distance between the collimator aperture and the face of scintillator **76** over distances ranging from directly adjacent, to typically 6 inches. For a 5  $\mu\text{Ci}$  Cd109 source, a collimator designed with 5 mm walls of tin works well. If higher frequency gamma sources such as Cs137 are to be tested, a lead (Pb) collimator should be used. In some embodiments there are advantages to construct the collimator with an aperture liner (not shown) made of a different element. Tested successfully were copper lined with tin, and lead lined with tungsten.

Channel 1 scintillator **76** must be specially designed to be thin enough to allow at least 10% of the incident gamma-rays to pass through. The most appropriate design is to use a standard thallium doped sodium iodide scintillator, NaI(Tl), cut as a square thin slab approximately 40 mm long and wide. The thickness is critical. The experiments for Figs. 8 and 9 have used this same preferred embodiment design with a 4 mm thick x 40 mm x 40 mm channel 1 detector. The slab is packaged and encased in thin aluminum foil, as standard in nuclear industry. Window **80** at the thin end of scintillator **76** couples light to PMT **82** at its flat photocathode window. Typically, PMT **82** will have a round face, and the drawing does

not indicate the true width and length of the PMT. Scintillator manufacturers can either make a scintillator with its own window **80**, or can connect it directly to a photomultiplier tube in a hermetically sealed light tight unit. Channel 2 scintillator **84** is typically a standard 1.5 inch diameter right cylindrical NaI(Tl) scintillator and is normally purchased permanently connected to PMT **86** (not drawn to scale). The aperture of collimator **72** must be narrow enough such that cone **74** does not extend beyond the far side of scintillator **84**. The collimator is necessary in all experiments. Another reason for collimating is to reduce scatter within a surrounding shield. The output signals from the photomultipliers are fed to preamplifiers **88** and **90** to amplify the signal approximately a factor of 10.

The preamplifiers should be located as close to the PMTs as practical. I found that a limiter feature was useful at the preamplifier stage to avoid artifacts; so I designed and built the preamplifier. Commercial preamplifiers did not have this feature. The simplest method of constructing the preamplifier is to use the LINEAR TECHNOLOGY CORP. LT1222 op-amp which includes the limiter feature, in a conventional inverting amplifier circuit. Signals from each channel are then fed to shaping amplifiers **92**, **94** to deliver shaped pulses that work in conjunction with timing-type single channel analyzers SCA1 **96**, SCA2 **98** to deliver digital timing pulses. I used the ORTEC 460 shaping amplifier, and the ORTEC 551 timing SCA, of common nuclear instrumentation use. Digital output from SCA1 **96** are counted by counter **100**, and digital output from SCA2 **98** are counted by counter **102**. Counts at counters **100**, **102** not in coincidence are called singles. In the experiments, counter **100** records singles rate  $R_1$  and counter **102** records singles rate  $R_2$ . The LECROY digital oscilloscope DSO **104** with its time analysis and

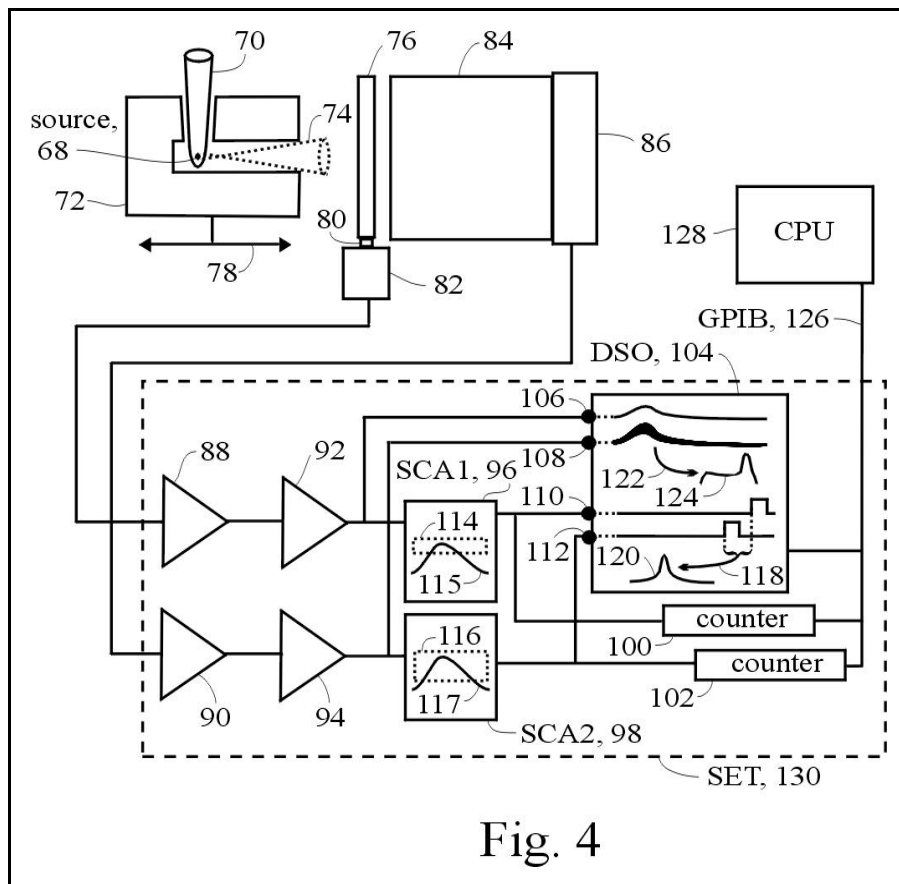


Fig. 4

histogram features was found to be the best way to instrument these experiments. Connections to DSO are: output of shaping amplifier **92** to DSO-BNC 1 **106** (BNC is a connector type), output of shaping amplifier **94** to DSO-BNC 2 **108**, output of SCA1 **96** to DSO-BNC 3 **110**, and output of SCA2 **98** to DSO-BNC 4 **112**. DSO **104** monitors the analog shaped pulses at DSO-BNC 1 **106** and DSO-BNC 2 **108** in storage mode to visually assure that falsely shaped pulses do not exceed ~1%. DSO-BNC 2 **108** is also useful for collecting analog pulse amplitudes for coincidence-gated pulse amplitude plots (histograms).

This DSO can record pulse-amplitude histograms and pulse shapes at the same time. In an initial setup procedure, trigger DSO from the SCA pulse on channel 3 **110** while adjusting upper and lower level SCA settings in an iterative process to obtain the desired window **114**. Then do similarly for the other window **116**. An SCA window is adjusted until the pulse-amplitude histogram shows the characteristic gamma-ray photopeak response  $\Delta E$ . An example of a window

width is shown at  $\Delta E$  64 Fig. 3. These windows 115 and 117 operate on shaped pulses from shaping amplifiers 92 and 94.

The histogram of times between SCA pulses 110 112 is a  $\Delta t$  plot 120. The DSO smart-trigger is set to trigger on DSO-BNC 3 only after DSO-BNC 4 has sensed a pulse within  $t_s$   $\mu$ s. In preparation for the  $\Delta t$  plot, delay settings on SCA1, SCA2, and the DSO must be performed. LT344 DSO histogram process 118 internally creates  $\Delta t$  plot 120 in response to the smart-trigger. In experiments examining coincidence gated pulse-amplitudes from channel 2 (the back scintillator), the smart-trigger 118 and a pulse-height histogram of channel 2 will create the spectra.

The system can be fully automated if counters 100, 102, and DSO 104 are equipped to communicate using the general purpose instrumentation bus GPIB 126 under computer CPU 128 control. The marked set of electronics, SET 130, is used to simplify the description of another preferred embodiment in Fig. 12.

## EXPERIMENTAL RESULTS USING TANDEM GEOMETRY

Many tests were performed with the same electronics as Fig. 4 but with different detectors and source collimator. The well-type scintillator 140 is described here because it is commercially available in contrast to the thin slab 76 of Fig. 4. The disadvantage of using a well-tube is that the source needs to be small to fit in a specially shaped collimator. The detectors and source holder of Fig. 5 were used for the experiment of Fig. 6; otherwise electronics and description for preferred embodiment of Fig. 4 apply. In Fig. 5, source holder 134 holds 5  $\mu$ Ci of Cd109 at its tip inside collimator 136 made of tin. Collimator 136 had a hole to let through cone 138 of gamma-rays to interact with two NaI(Tl) scintillators. Scintillator 140 of channel 1 was a 42 x 42 mm cylindrical well-type, with a 17 mm cylindrical hole through its side to accommodate collimator 136. Cone 138 passed through a short wedge of scintillator 140 ranging from 3 to 5 mm of NaI(Tl) scintillation material. Radiation of cone 138 continued to channel 2 scintillator 142, a 2 x 2 inch BICRON

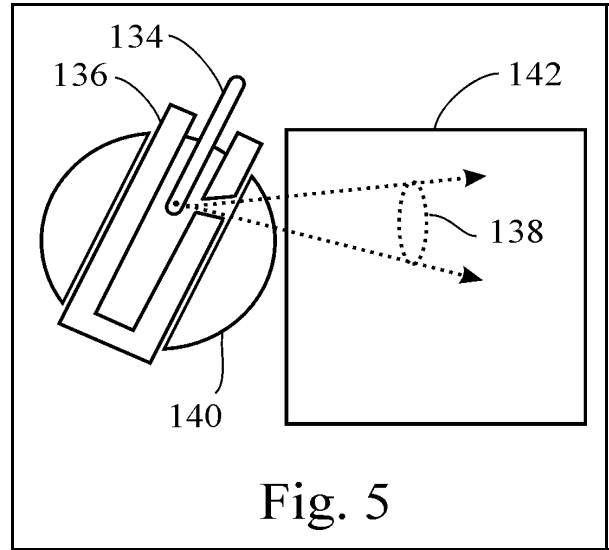


Fig. 5

brand NaI(Tl) with an integral PMT (not shown). Gamma-rays in cone 138 must pass through scintillator 140 to get to scintillator 142.

In the experiment for Fig. 6, performed July 5, 2004,  $\Delta t$  plot DA using Cd109 gave good resolution. Plot DB was a  $\Delta t$  plot with source and holder 134 removed to see pairs due to background. For both plots the window of trigger time 148 was set at  $t_s = 2$   $\mu$ s, as marked. Fig. 6 is a section of screen capture from the DSO with some added annotation. The DSO screen capture

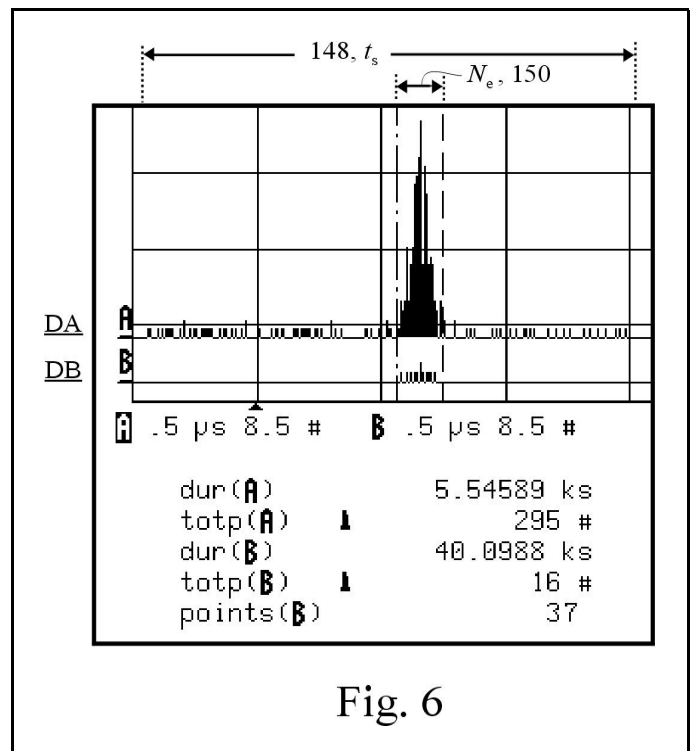


Fig. 6

shows: dur(A) the duration of plot **DA**, totp(A) the total number of detection events in plot **DA**, and (B) the plot **DB**. A section of bins  $N_e$  **150** were used to count the unquantum effect. In plot **DA** the coincidence effect **150** stands above the randomness, I call the wings. In plot **DB** coincidences caused by background radiation show only  $16/40.1 \text{ ks} = 4E-4/s$ , an average of one count every 1.4 hours. This small background coincidence rate is most likely due to cosmic ray showers and will be subtracted from the rate read from section  $N_e$  in plot **DA**. After correcting for background, any rise in the count per time range in section  $N_e$  above the count per time range in the surrounding wings of the  $\Delta t$  plot is a quick way of seeing that chance is surpassed. That is, any peak in this  $\Delta t$  graph indicates exceeding chance. The experimental coincidence rate is

$$R_e = (295/5.5\text{ks} - 16/40.1\text{ks}) = 5.3E-2/s.$$

The chance coincidence rate  $R_c$  is calculated from the singles counters and  $\tau$  by Eq. (11).

$$R_c = \tau R_1 R_2, \quad \text{Eq. (11)}$$

Equations (10) and (11) are found in GF Knoll's *Radiation Detection and Measurement*. With both SCAs similarly windowed around 88 keV the singles counters and  $\tau$  gave

$$(R_1 = 291/s)(R_2 = 30/s)(\tau = 0.2\mu s) = 1.74E-3/s = R_c$$

$$R_e/R_c = 5.3E-2/1.74E-3 = 30.4 \times \text{chance.}$$

This is the unquantum effect.

It was very important to show that the unquantum effect was not a special case of using Cd109. Another experiment (not shown) using Co57 using a lead collimator in the well-tube on channel 1 gave 190 times chance. Lead has a fluorescence at 87 keV and care was taken to avoid windowing near this part of the spectrum when using Co57. This is why I do not use lead for the collimator with Cd109. I performed many experiments with Co57, some with tungsten lined collimators and all with similar results. Some experiments have employed an aluminum filter mounted at the aperture of the

collimator to reduce x-rays. No difference has been noticed from this practice.

Fig. 7 shows  $\Delta t$  plot **EA** using Cs137, a signal generator plot **EB**, and a long time  $\Delta t$  plot **EC** using Cd109. These early experiments were performed August 2003 and used a time-to-analog converter fed to a multichannel analyzer. Plot **EA** was a search for an unquantum effect using a higher frequency gamma-ray. Experiment of plot **EA** used: 1  $\mu\text{Ci}$  of Cs137 in a lead collimator, a 1 inch dia NaI(Tl) on channel 1, a 2 inch dia NaI(Tl) on channel 2, both SCA windows set to the 662 keV characteristic gamma-ray region, and a 10.5 hour duration. Plot **EA** showed only random times between events. This failure to read the unquantum effect is important for comparison to a later success where the necessary conditions were discovered. Plot **EB** is a control experiment to generate random pairs, using a signal generator in coincidence with a Cd109 source. Plots **EA** and **EB** are what physicists usually see. These were important controls to check Eq. (11).

Returning to the issue of energy conservation, there is a way to test that my effect upholds it. If there are events triggered by the gamma in coincidence, it should remove events from the random distribution in the wings of the  $\Delta t$  plot. This test was attempted in a 4.8 day long test shown of plot **EC**, using hardware of Fig. 5 and a time-to-analog converter. The peak-section **160** accounted for 0.6 of all counts on plot **EC**, but the fraction in the unquantum effect was only  $\sim 1/300$  of the total true start-counts. The measurement revealed a slight lowering of the count in the wings but this lowering did not surpass the quantity in my error analysis. The experiment should be repeated with refinements to verify energy conservation,

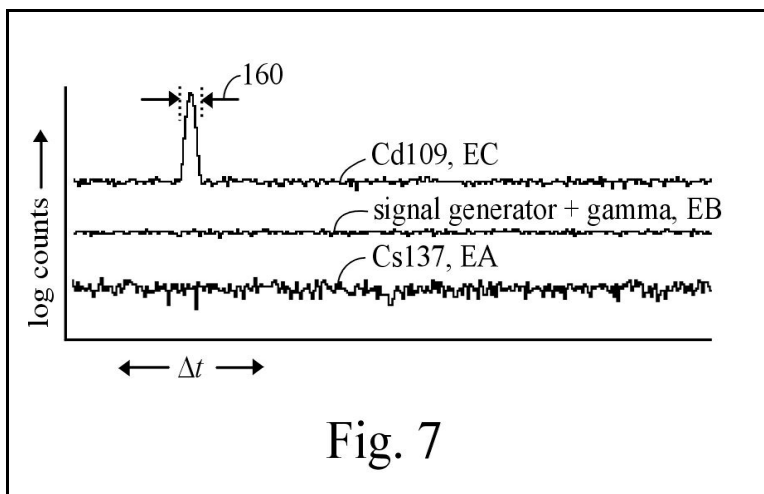


Fig. 7

even though we fully expect energy to be conserved.

Though my early tests with Cs137 revealed no unquantum effect, I have on August 18, 2004 discovered how to reveal the effect using my specially made thin detector. The hardware for data of Fig. 8 was the same as that of the preferred embodiment of Fig. 4 with these specifications: the 4 mm NaI(Tl) on channel 1, a 42 x 42 mm NaI(Tl) on channel 2, and a collimator made of a 2 inch thick lead block with a 1/2 inch diameter hole to accommodate a purchased 1 μCi test-tube source of Cs137. The collimator remained fixed and the source was retracted within the collimator to different distances from the channel 1 detector. In plots of Fig. 8 the duration of experiments and vertical scalings are different, but they are still valuable for seeing how the unquantum effect appears above randomness. Horizontal time scale is 500 ns for the full width shown in each plot. Plot FA shows background coincidences with no gamma source at a total of  $260 \times 10^{-6}/s$  in a 10 bin section 166. For plot FB the source was 1 inch from the detector, and shows only randomness, as expected by quantum mechanics. For plot FC the source was at 2 inches with the same result. For plot FD the source was at 3 inches, and an unquantum effect begins to appear. For FD, within section 166  $R_c$  measured at only 1% above chance, calculated by singles counters, and after subtracting background. For plot FE at 3.5 inches, duration 84.4 ks, the unquantum effect ratio calculates to 1.6 times chance. Since Cs137 decays by a beta decay process, this shows the unquantum effect is not limited to an electron capture process. The small unquantum effect read from Cs137 is consistent with the theory of linking the effect to detector photoelectric effect efficiency. In plot FF the lead was rearranged such that the gamma-rays needed to pass uncollimated and through 1 inch of lead the detectors. Comparing the distance to the lead effects:

At 3.5 inches,

$$R_1 = 12.4/s, R_c = 20 \times 10^{-6}/\text{bin-sec}, R_c = 12.4 \times 10^{-6}/\text{bin-sec}, R_c/R_c = 1.61.$$

Through 1 inch of lead,

$$R_1 = 21.7/s, R_c = 26 \times 10^{-6}/\text{bin-sec}, R_c = 15.4 \times 10^{-6}/\text{bin-sec}, R_c/R_c = 1.68.$$

This important test shows that the unquantum effect can be manipulated to appear by adjusting distance and by matter-filter. I did not control closely to maintain similar singles count rates with distance, but it was done (previously) in the next-described test.

Fig. 9 shows data taken July 2004 using: the same detectors used for Fig. 8, the electronics of Fig. 4, and a 1 μCi Co57 source collimated with a 1/8 inch diameter 1/4 inch thick lead aperture. The source and collimator moved as a unit as prescribed in Fig. 4. Horizontal time scale is 1 μs/division, and the DSO smart-gate time window was  $t_s = 2 \mu s$  as shown.

Plot GA shows background at  $421 \times 10^{-6}/\text{sec}$  in a 26 bin effect-section and was used to subtract its rate from data of the remaining plots. Plot GB had the source to detector distance at 1/2 inch and revealed 22.5 x chance. Plot GC at 1 inch revealed 9.3 x chance. Plot GD collecting data for 34 hours at 1.5 inches revealed 11.6 x chance. Here at 122 keV from Co57 the unquantum effect was generally stronger with the source close to the detectors.

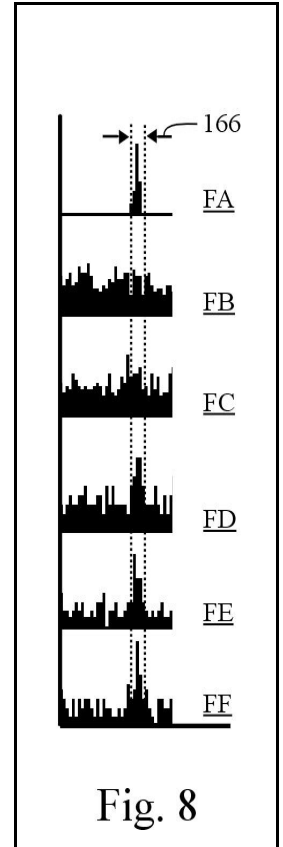


Fig. 8

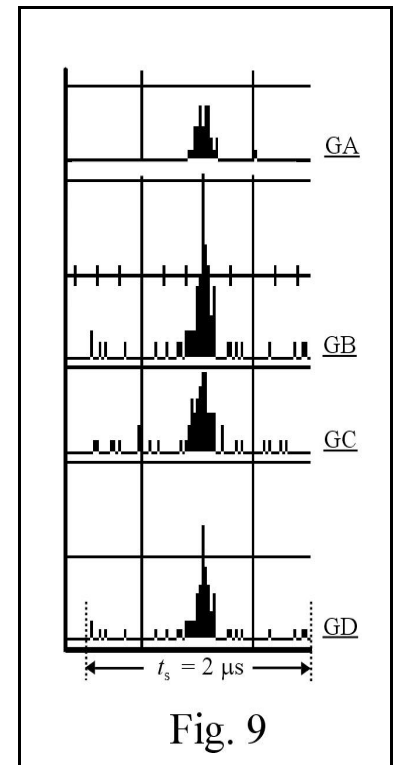


Fig. 9

With 122 keV when the source was moved back, the unquantum effect was lower. The singles rate did not lower because the collimated radiation cone was within both detectors in both cases. Now compared to the 662 keV gamma, when the source was moved back, the unquantum effect was enhanced. Also 662 keV, for the test adding Pb, the unquantum effect was enhanced. We conclude that each gamma-ray wavepacket is made to spread-out in each case. Scattering through matter has the same effect as a spreading wave. The whole of these tests indicate that each  $h\nu$  is emitted at a solid angle that narrows as a function of frequency, as expected from classical optics. We conclude that when the  $h\nu$  cone's area matches the microscopic absorber, it optimizes the unquantum effect. There are two kinds of radiation cones: a microscopic cone set by  $h\nu$ , and a macroscopic cone set by the collimator. It is best to move the source and collimator as a unit to aid these investigations. Only the characteristic spectral sections (the photopeak) were windowed and not the Compton sections.

Tests in with the 59 keV of Am241 did not reveal any unquantum effect (of August 2004 not shown). NaI(Tl) and a 3/4 inch thick CsFl(Eu) scintillator were tested in various configurations. CsFl(Eu) was chosen because of its greater transparency at this lower gamma frequency. These measurements offer clues to the classical structure of an individual  $h\nu$  pulse, and have only been given an initial exploration here. The common factors among these experiments indicate that a high pulse amplitude resolution due to a high photoelectric effect efficiency at the detector work best. These methods of reading spatial and temporal properties of singly emitted  $h\nu$  are not at all understood from the photon model.

So far Cd109 and Co57 are the only sources that have revealed a strong enough unquantum effect to be useful as a probe upon a material scatterer. Compared to an x-ray  $h\nu$ , an Am241 gamma from alpha decay is expected to be more pulse-like and have a narrower solid angle. Since our tests found such a poor unquantum effect with Am241, it is unlikely that an x-ray source would display the effect, but it remains to be tested. The failure of the photon model for gamma-rays, the

most particle-like kind of light, implies the entire electromagnetic spectrum is purely classical.

Data for Fig. 10 is from my test of May 9, 2003 using the NaI(Tl) well-tube detector at channel 1 in tandem with an HPGe detector at channel 2. My 5  $\mu$ Ci of Cd109 was inside the well-tube with a copper collimator insert. The channel 2 SCA window was widened to observe a higher spectral section of what passed through in coincidence. Detector orientation was the same as shown in Fig. 5 and was inside the giant Pb shield. Plot HA is a singles spectrum from the HPGe, and was useful for calibration because the 264 keV peak from Cd113m was present. Plot HB is a coincidence-gated pulse amplitude plot, whereby the triggering was accomplished with one-shot pulse generators feeding an ORTEC 414A coincidence module to overlap 100 ns pulses. The 414A gated a multichannel analyzer to record pulses from the channel 2 shaping amplifier via an analog delay line. The final timing adjustment to overlap two 100 ns pulses was aided by a test with Na22. I took special care to eliminate distorted pulses from the channel 2 detector by building a high speed pile-up rejector of my own design

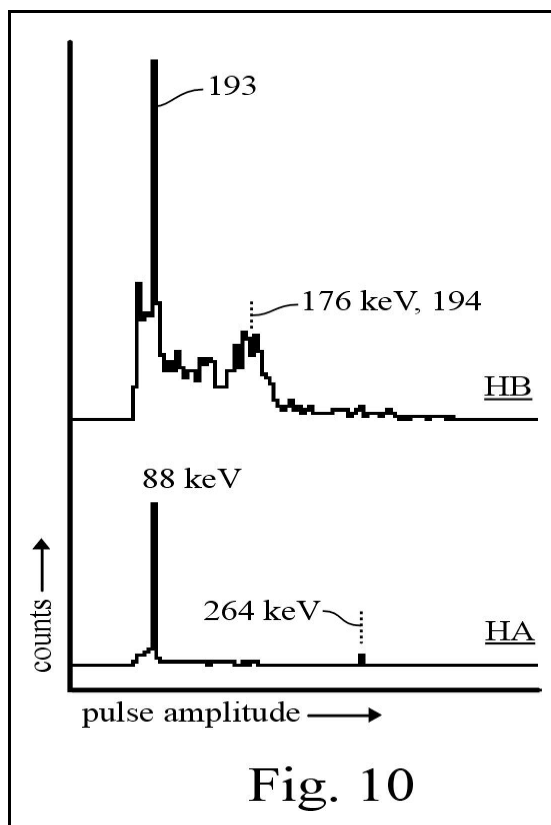


Fig. 10

using a tape shape-mask on the CRT. Coincidence-gated pulses of non-standard shape were filtered from entering data to plot **HB**. Pile-up elimination was always less than 1% of the recorded coincidences. It was later determined that this low rate of false pulses would not significantly affect the gated pulse amplitude plot and resulting statistics. Therefore this pile-up rejector technique was used only on this experiment. The LT344 DSO monitored all pulses, and it was found that this was a better way to read any form of distortion, even forms a good pile-up rejector would miss. Plot **HB** reveals a sensational coincidence-gated peak **193** only one bin wide at 88 keV.

$$R_c = 273/1289s = 0.00562/s$$

$$R_c = 2 R_1 R_2 \tau = 2(3/s)(1289/s)(100ns) = 0.000773.$$

Therefore chance is exceeded by

$$R_e/R_c = 0.00562/0.000773 = 7.26.$$

At 2 x 88 keV the gated plot **HB** clearly shows a feature not present at all in the singles spectrum: peak **194** at 176 keV. I predicted this 176 keV peak from my single detector sum-peak analysis of an anomalous shelf, section **60** Fig. **3**. For this I calculated ~200 x chance.

I first observed coincidence-gated unquantum effect plots in a similar manner using Cd109 and two NaI(Tl) at July 2002.

If some contamination source such as a gamma from Cd113m were to generate a pair of events in coincidence by Compton scatterings, a broad spectrum would be present at 88 keV, point **193** in plot **HB**. The incredible gated single bin peak **193** of plot **HB** shows this is not the case. This eliminates any argument against a contaminant causing the unquantum effect.

Continuing with tandem geometry, test results begun July 11, 2004 are shown in Figs **11A** and **11B**. Orientation of components are the same as Fig **5**, and electronics are the same as Fig **4**. The NaI(Tl) well-type scintillator was on channel 1 in tandem with a 2 inch NaI(Tl) on channel 2. Here the LT344 DSO was used to simultaneously generate both the  $\Delta t$  and coincidence-gated pulse amplitude plots. To obtain good pulse-amplitude data, time window  $t_s$  was narrowed to 300 ns to exclude most of the random response (the wings). Full

horizontal scale shown for Fig. **11A** is 350 ns. Fig. **11A** are  $\Delta t$  plots using three preparations of  $^{109}\text{Cd}$  for sources.

Plot **IA** used the same 5  $\mu\text{Ci}$  preparation of  $^{109}\text{Cd}$  as used in other experiments here of this specification. This source was prepared in a glass tube melted and drawn to a sharp depression. A ten  $\mu\text{Ci}$   $^{109}\text{CdCl}_2$  (cadmium chloride) aqueous solution was dropped in and evaporated to leave a narrow salt deposit. This being about a year old and encased in glass made it ~ 5  $\mu\text{Ci}$ .

For plot **IB**  $^{109}\text{Cd}$  was specially prepared by electroplating a  $^{109}\text{CdCl}_2$  solution onto a thin platinum wire, depositing approximately 29  $\mu\text{Ci}$  of metallic  $^{109}\text{Cd}$ . In plot **IC** the  $^{109}\text{Cd}$  was specially prepared by evaporating a  $^{109}\text{CdCl}_2$  solution, but this solution also had sulfuric acid and NaOH added. These chemicals were from what was left over in the electroplating solution, but proved even more useful in making a potent  $^{109}\text{Cd}$  salt source. The solution was evaporated in a centrifuge tube to deposit about 1  $\mu\text{Ci}$  of a complex  $^{109}\text{Cd}$  salt. It took much work in January to June 2004 to optimize these electroplating and salt depositing

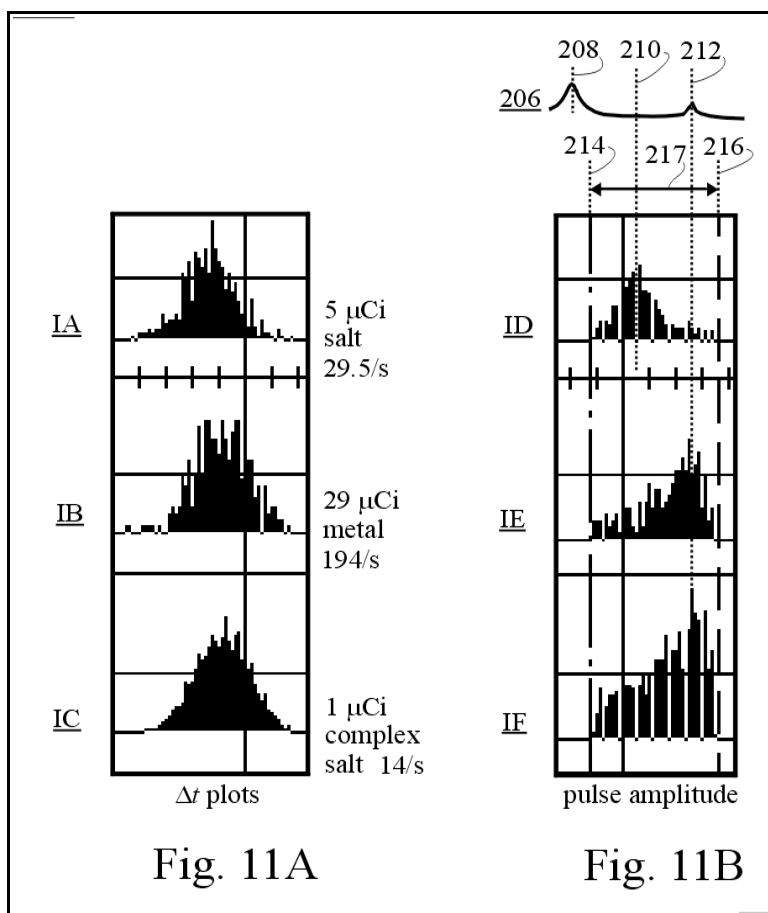


Fig. 11A

Fig. 11B

processes. A servo loop monitored current in the plating process to perfectly control a motor to position the platinum wire, just breaking the solution surface.

The rates from the well-type scintillator for channel 1, windowed around the 88 keV gamma response are posted to the right of Fig. **11A**, and give evidence of the lower  $\mu\text{Ci}$  of the complex salt. The degree above chance for each experiment was calculated as previously described.

Plot **IA** 5  $\mu\text{Ci}$  in salt-form gave  $R_c/R_c = 70$ ,

Plot **IB** 29  $\mu\text{Ci}$  metal form gave  $R_c/R_c = 94$ ,

Plot **IC** 1  $\mu\text{Ci}$  complex salt gave  $R_c/R_c = 3853$ .

Fig. **11B** are coincidence-gated pulse amplitude plots using the same sources as in Fig. **11A**: the 5  $\mu\text{Ci}$  salt **ID**, 29  $\mu\text{Ci}$  metal **IE**, and 1  $\mu\text{Ci}$  complex salt **IF**. A reference spectrum of  $^{109}\text{Cd}$  was acquired for this test, but is only drawn here **206**. Point **208** marks 1 x 88 keV, **210** marks 2 x 88 keV, and **212** marks where 3 x 88 keV events would be detected. Plots of Fig. **11B** are aligned to the same horizontal scale. SCA2 set lower level **214** and upper level **216** for these plots, defining SCA2 window **217**.

Plot **ID** shows a trend of two pulses that overlapped in coincidence at mark **210**, indicating two events in the channel 2 detector, plus one in the well detector: a three in-coincidence unquantum effect.

Plot **IE** shows a coincidence peak at mark **212** indicating that three events must have piled-up more often than two events and that this happened in addition to the gamma-triggered event in the channel 1 detector; adding to a 4 events-in-coincidence unquantum effect. A similar analysis holds for plot **IF**.

Comparing plots **ID** and **IF** shows that perhaps less, but not more  $\mu\text{Ci}$ , can bring out the 3 x 88 keV effect. Comparing plots **ID** and **IE** shows that a change to the metallic state and more  $\mu\text{Ci}$  can bring out the 3 x 88 effect. Comparing plots **IB** and **IC**, we see that the complex salt was extremely potent in producing coincidences surpassing chance. This is my best: 3853 times better than chance. An enhanced unquantum effect with salt compared to the metallic form of  $^{109}\text{Cd}$  was confirmed in several other tests, including tests windowed only at the photopeak.

Conventional gamma spectra were taken, and a careful comparison between the metallic  $^{109}\text{Cd}$  used for plot **IB** and the complex salt  $^{109}\text{Cd}$  used for plot **IC** showed no difference other than overall activity. These tests also confirm that the  $^{113\text{m}}\text{Cd}$  used in plots of experiment **IA**, **ID**, and in previous experiments, does not play a role in causing coincidences at 264 keV (3 x 88) spectral position. Plot **ID** had a 2 x 88 response instead of a 3 x 88 response.

My success in electroplating  $^{109}\text{Cd}$  led to the discovery that the metallic  $^{109}\text{Cd}$  in most experimental arrangements revealed lower unquantum effect potency compared to the same experiment with a salt  $^{109}\text{Cd}$ . This leads to a new way to use the unquantum effect. Mixtures and crystalline state of matter at the source affect the classical emission properties of the gamma-ray. There was pre-existing evidence of a related effect published in "Comparison of the values of the disintegration constant of  $\text{Be}^7$  in Be, BeO and  $\text{BeF}_2$ " *Physical Review* 90 (1953) pg. 610 by JJ Kraushaar et al, where the decay rate of a beryllium isotope in an electron capture process can be modified by its chemical state. Their effect was very small and difficult to observe. My discovery similarly **links a chemical-state effect to nuclear electron capture**, but reads the effect much easier.

## PREFERRED EMBODIMENT USING BEAM-SPLITTER GEOMETRY

Fig. **12** is an arrangement for testing the unquantum effect in a beam-splitter geometry. Typically, a Cd109 source is used. Source **220** resides in holder **222**, and collimator **224** directs a beam of gamma-rays in cone **226** toward the channel 1 NaI(Tl) scintillator **228**. The primary purpose of using a collimator in beam-splitter geometry is to shade the channel 2 detector **232** so that it only receives gamma-rays from scatterer **230**, a material under study. Detector **232** must not receive radiation directly from source **220**. Another reason for collimating the beam is to reduce radiation scattering from within a surrounding shield. The shield should be lined with at least 2 mm of sheet tin. This thin Sn by itself was tested to be adequate for some

experiments, but the experiments here were all done in my Pb shield lined with Sn and Cu. Scatterer **230** is placed in cone **226** as close to source **220** as possible. The object of this Fig **12** test is to see if the unquantum effect changes with angles  $\Phi$ ,  $\Theta$ ,  $\rho$ . A change with angle would reveal properties of the scatterer. This apparatus was constructed and has delivered data, but has not yet articulated axis  $\rho$ . In tests, an example of which is described in Fig. **13**, a good setup was found: source **220** of 29  $\mu\text{Ci}$  Cd109 refined by electroplating onto a  $\sim 0.001$  inch platinum wire (not shown), collimated radiation cone **226** with 20 degree spread, collimator **224** made of a 3 cm cube of copper with a tin aperture (not shown) molded and machined to define cone **226**, and distance from source **220** to scintillator **228** at 8 cm. These specifications are not critical but they influence each other. The minimum angle of cone **226** depends upon the distance to scintillator **228**, the strength of source **220** and the duration of the experiment. Source **220** is best prepared to be as physically small as possible to work with collimator **224** to maximize the radiation flux within cone **226**. The small source has a great advantage in the ability to create a narrow radiation cone with a weak source, while remaining exempt from license requirements. Scatterer **230**, best shaped as a sphere 1 to 3 cm in diameter, is a sample of material under study placed to intersect cone **226**, and placed as close to source **220** as possible; best within 2 cm. A sphere will not introduce an attenuation artifact due to material thickness when changing orientation. If  $\rho$  is not articulated a cylinder will work well. A flat plate can work with the understanding that an angle adjustment will vary gamma-ray transmission. Axis **234** is through the center of cone **226**,  $\Theta$  is the angle for rotatating scintillator **232**,  $\Phi$  is the angle of rotating scatterer **230** about axis **234**, and  $\rho$  is the angle for rotatating scatterer **230** against axis **234**.

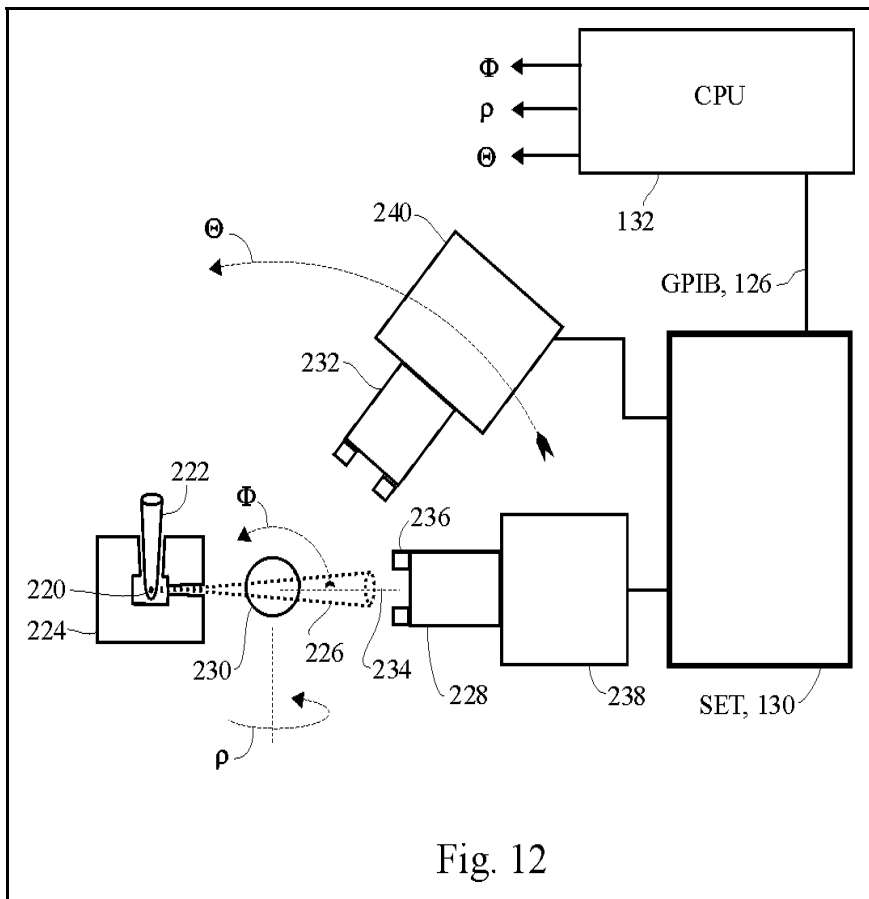


Fig. 12

In future implementations, experimental run times can be shortened by using a stronger radioisotope source or miniaturizing the entire apparatus. Closely related is the desire to narrow cone **226** to enhance angle resolution.

To aid in defining narrower angle ranges, aperture blocks **236** (one of 4 labeled) of an appropriate gamma blocking material may be placed to narrow the exposed area of scintillators **228** and **232**. Scintillators **228**, **232** are coupled to photomultiplier tubes **238**, **240** in the usual manner to create gamma detectors. Signals from photomultiplier tubes **238**, **240** are wired to electronics SET **130** as outlined for Fig. **4**. SET **130** interfaces to CPU **132** computer bus **126**, to perform motion controls (not shown) upon angles  $\Phi$ ,  $\rho$ , and  $\Theta$ . A perfected measurement would deliver a matrix of coincidence data verses angles. Angle rotation should be incremental.

## EXPERIMENTAL RESULTS USING BEAM-SPLITTER GEOMETRY

I have performed scattering tests with different sources, scatterers, geometries, detectors, applied fields, angles, and temperature, all defying the principle of the photon. Fig. 13 shows data from May 11, 2004. The arrangement of components is similar to Fig 12 and was inside the 1 ft diameter Pb shield. Source was the 29  $\mu\text{Ci}$  Cd109 electroplated platinum wire mounted inside a copper block with a tin conical aperture to define cone 226 of Fig. 12. I tested the cone radiation to be about 20 degrees wide. At the aperture of the collimator was a filter of 2 mm aluminum to attenuate  $K\alpha$  x-rays. The channel 1 detector was a 1.5 inch diameter BICRON NaI(Tl) 8 cm from the scatterer and positioned to optimize capture of undeflected gamma-rays. The channel 2 detector was a 3 inch diameter BICRON NaI(Tl) placed 8 cm from the scatterer, with  $\Theta = 60$  degrees. Both SCAs were set to window the characteristic 88 keV gamma section. The scatterer was 21 silicon wafers 4 cm diameter in a stack 6 mm thick. These were clean wafers of the type used in semiconductor manufacture, with its orienting flat placed toward the channel 2 detector. The scatterer was mounted to pivot on axis  $\Phi$ .

Fig. 13 is a section of an LT344 DSO screen capture with my added annotation. Section 248 reads  $\tau$  and  $R_e$ .

**JC**  $\Delta t$  plot is background coincidences accumulated over 58 ks of rate  $3.6\text{E-}4/\text{s}$

**JB**  $\Delta t$  plot are coincidences accumulated over 65 ks with the scatterer mounted for gamma-rays  $60^\circ$  from its flat surface and also with  $\Phi = 30^\circ$ , as if to reflect like a mirror to detector 232.

$$R_c = R_1 R_2 \tau = (27/\text{s})(9.5/\text{s})(100\text{ns}) = 1.9\text{E-}4/\text{s}.$$

$$R_e = (36/65\text{ks}) - (3.6\text{E-}4/\text{s}) = 1.9\text{E-}4/\text{s}.$$

$$R_e/R_c = 7.4 \text{ x chance.}$$

**JA**  $\Delta t$  plot are coincidences accumulated over 37.5 ks with the scatterer mounted with its plane perpendicular to the incident gamma-rays:  $\Theta = 0^\circ$ ,

$$R_c = (4.2/\text{s})(6.1/\text{s})(120\text{ns}) = 3.1\text{E-}6$$

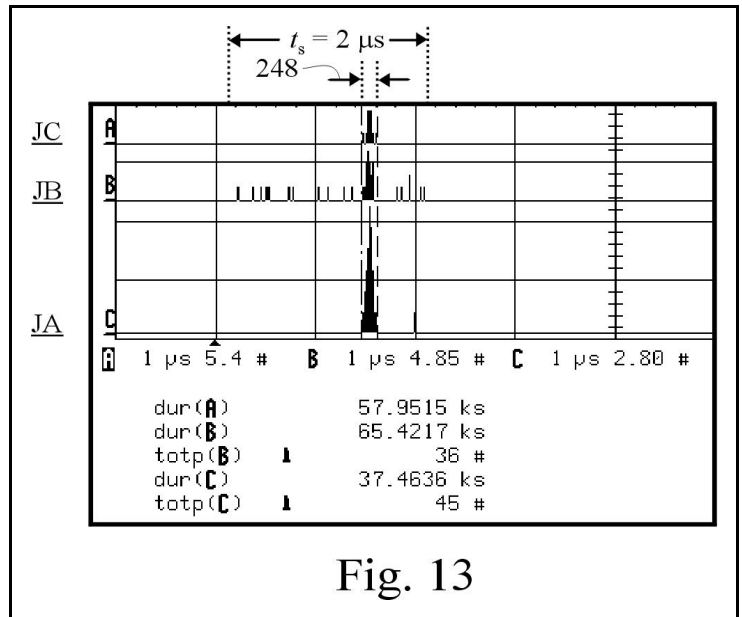


Fig. 13

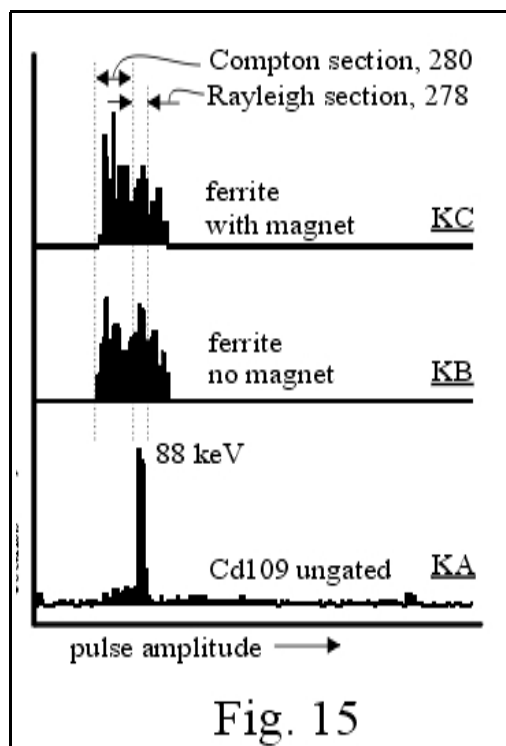
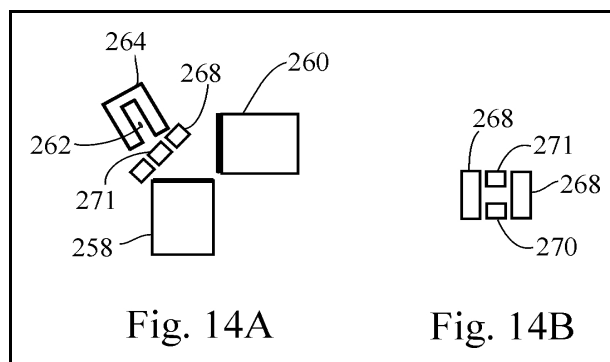
$$R_e = (45/4.6\text{ks}) - (3.6\text{E-}4/\text{s}) = 9.4\text{E-}3/\text{s}$$

$R_e/R_c = 3000 \text{ x chance.}$  Rotating the scatterer caused an unquantum increase of 400. Notice that even with less material in the way the singles rates  $R_1 R_2$  without the wafers twisted were lowered, indicating radiation was diverted. Also, the effect was not enhanced by the wafer surfaces acting like mirrors, indicating a volume effect. Either the orientation of atomic or electronic layers must be at play. In silicon the spacing between atoms is  $d = 0.313 \text{ nm}$ , but the wavelength of 88 keV gamma is  $\lambda_{88} = c/v = hc/hv = (4.41 \times 10^{-15} \text{ ev-s})(3 \times 10^8) / (88 \text{ keV}) = 0.015 \text{ nm}$ . To deflect  $\Theta = 60^\circ$ , the perpendicular of an internal Bragg plane to the incident ray would be  $\Theta/2$ . Solving the Bragg equation,  $n\lambda = 2d \sin \Theta/2$  for the integral number of wavelengths gets  $n = 36$ . Inserting the next  $n$  at  $n = 35$  in the Bragg equation gets  $\theta = 57^\circ$ , a difference of  $3^\circ$ . However the solid angle of the cone of incident radiation was much wider at  $\sim 20^\circ$ . With our large channel-2 detector, any Bragg resonance would have completely blurred out. Therefore, this is not a Bragg reflection between atomic planes. It is Bragg reflection between charge-wave envelopes, a spacing close to the gamma-ray wavelength. This concept is in our derivation of Compton effect, explained in THEORETICAL BACKGROUND.

In this test of Fig. 12 the metallic Cd109 worked well when the scatter angle was adjusted. The salt form of Cd109 worked well for seeing this chemical state change. We suspect that the coherence of the classical gamma-ray is at play.

The next three experiments with data in Figs. 15, 16, and 18 all use two HPGe detectors for coincidence-gated pulse amplitude experiments performed October 2003. The same preamplifiers, shaping amplifiers, SCAs, and LT344 DSO were used. However in these tests a separate coincidence module set to 400 ns was used to gate the DSO. The DSO monitor both channels of each coincidence-gated pulse shape to insure that pile-up and ringing were not present. The channel 2 detector received gamma-rays deflected by a scattering material and its pulse height spectrum was recorded. The 5  $\mu$ Ci source of Cd109 was encased in a copper collimator that released a 40 cone  $\sim$ 40 degrees. A typical window of frequencies (freq = pulse height = eV) used in the channel 1 detector is marked  $\Delta E$ , 32 in Fig. 2. By windowing SCA2 to include the lower frequency Compton events, these tests can measure both Compton and Rayleigh scattered gamma-rays in coincidence with the undeflected ray. Rayleigh scattering, often called coherent scattering, is a change in direction with no wavelength increase and no Doppler charge-wave recoil. The deflected ray SCA2 lower level cannot be made too low or it will void the unquantum argument. With too low a level a gamma can split at the scatterer, obey  $E = hv$  and put one fraction of its frequency in the transmitted ray and the remaining fraction of its frequency in the deflected ray, thereby allowing one to invoke the principle of the photon to cause coincidences. The goal of this invention is to specifically avoid that scenario. The spread of pulse amplitudes from the detector needs to be taken into account, and this is a good reason to perform this kind of test with two HPGe detectors. Define  $E_{H1} = \{ \text{pulse amplitude in channel 1 at the high level of SCA1} \}$ , similarly  $E_{L1}$  for the low level, and for SCA2 write  $E_{L2}$ . In every experiment the criteria must be met that  $E_{L2} + E_{L1} < E_{H1}$ , otherwise the frequency could be lowered in a fluorescence process to cause true coincidences, not in violation of the photon model. A required step

in these tests is to ensure that the coincidence-gated rates break chance, by doing a chance calculation of singles rates with this widened



window.

A comparison of magnetic effects using a ferromagnetic and a paramagnetic material scatterer was performed using this coincidence-gated pulse amplitude technique. Components are shown in Figs. 14A: channel 1 HPGe 258, channel 2 HPGe 260, 5  $\mu$ Ci Cd109 source 262, collimator 264, magnetic conductive bars 268, neodymium magnet 270, 1.5 cm cube scatterer 271. Fig. 14B shows the magnet assembly as seen from source 262. It was designed so that the magnets could be removed for a control experiment. Hardware of Figs. 14A and 14B were used for the data of Figs. 15 and 16.

For data of Fig. 15, scatterer 271 of Fig. 14A was a cube of ferrite. Fig. 15 plots are ungated reference spectrum **KA**, gated no-magnet spectrum **KB**, and gated with-magnet spectrum **KC**. The calculation uses 12 bins of a Rayleigh section 278, and 256 bins of a Compton section 280. Calculating counts per bin-second, the Rayleigh/Compton =  $P$  ratio of rates from non-magnetized plot **KB** was 1.08, and from the magnetized plot **KC** was 0.76, giving  $P_{\text{magnet}}/P_{\text{nomagnet}} = 0.70$ . This is a 42% shift toward the Compton section with the magnet. With no magnet, Compton scattering is comparable with Rayleigh, indicating unbound charge in this substance. Charges were pushed by the gamma as much with and without the magnet. With the magnet there were more scattering sites shifted to the free charge-wave, as expected for a ferromagnetic material.

For data of Fig. 16, scatterer 271 of Fig. 14A was a cube of diamagnetic graphite carbon. Plots are coincidence-gated pulse amplitude **LA** with no magnet, and **LB** with magnet. Calculations use Rayleigh section 286, and Compton section 288. The time duration (dur) of the experiment and counts (totp) for the Compton shifted section are in the DSO screen capture. I conservatively took Rayleigh section 286 at 6 bins wide, measured ratios Rayleigh/Compton =  $P$ , and took the ratio for both cases to get  $P_{\text{magnet}}/P_{\text{nomagnet}} = 1.4$ . With the diamagnetic carbon there was a 40% enhancement of Rayleigh scattering with the magnet. With the magnet, the Compton downshifted section was suppressed. Rayleigh implies non-moving stiff charge-beats, as expected with a diamagnetic.

AH Compton attempted to measure an effect of a magnetic field on gamma scattering in "The nature of the ultimate magnetic particle" *Science* Vol. XLVI, no. 1191, pg. 415, Oct. 26, 1917. His failure to see evidence for his ring electron model was part of what led him and modern physics to abandon the ring electron in favor of the point electron. Compton's 1917 work was similar to mine of Figs 15, 16, but with x-rays and no coincidence apparatus. My positive magnetic influence is consistent with Compton's original ring electron model.

With a ferromagnetic substance, the magnetic field enhanced Compton scattering. With carbon, a diamagnetic substance, the magnetic field

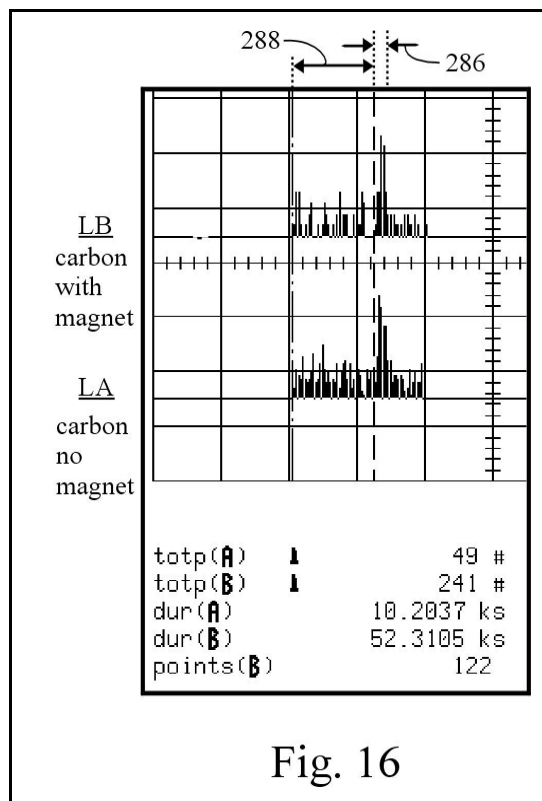


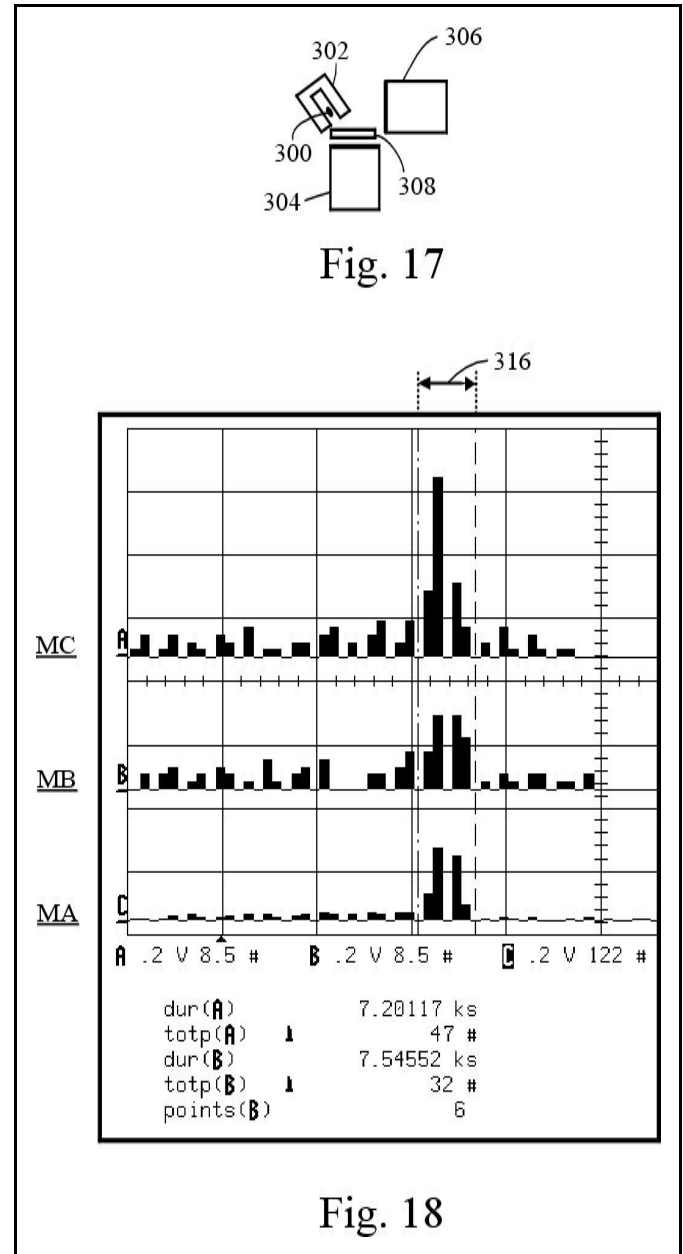
Fig. 16

reduced Compton scattering. Relating the degree of recoil motion of the charge-wave to these magnetic properties offers a new kind of material science probe with the ability to sort out stiff and flexible chemical bond structures. The magnetic field used in these tests was of the order of 0.1 T. From a cyclotron resonance calculation I had performed using pair creation, I was able to calculate for the proton that its magnetic field is about  $8 \times 10^6$  T at a radius of  $1 \times 10^{-14}$  m. Then using a  $1/r^3$  calculation, 0.1 T would be the strength at about 0.2 Bohr radius. Using calculations of this sort one can determine the radius of the scattering site as a function of magnetic field strength. Tests like those for Figs. 15 and 16 can be performed over a range of field strengths, and angles, to reveal the shape and nature of atomic bonds.

Figs. 17 and 18 refer to an experiment on how temperature alters a coincidence-gated pulse amplitude spectrum using 88 keV gamma-rays. Fig. 17 shows the 5  $\mu$ Ci Cd109 source 300, in copper collimator 302, directing gamma-rays to channel 1 HPGe detector 304. Channel 2 HPGe detector 306 receives scattered gamma from

scatterer **308**. Scatterer **308** was a 2 x 6 x 3/8 inch slab of aluminum. The lower 3 inches of the Al slab was in a styrofoam tub of liquid nitrogen (LN). The upper 3 inches in the gamma-ray path was wrapped by 1/4 inch Styrofoam to prevent ice formation. Components remained in place for an accurate comparison of with/without LN. The cold test ran ~ 1.3 hours, and the room temperature test ran ~ 1.1 hours. A temperature sensor was also employed. Fig. **18** is a section of screen capture from the LT344 DSO with surrounding annotation, and shows plot **MA** of a Cd109 singles spectrum for reference, plot **MB** coincidence-gated pulse amplitude plot with the Al at room temperature, plot **MC** coincidence-gated pulse amplitude plot with the Al cooled by LN, and section **316** of 6 bins used in the calculation. A remarkable effect is readily seen upon comparing peak sections of plots **MB**, **MC**. At half-maximum amplitude, the peak section narrowed a factor of 1/3 when cooled. There were no other physical or instrumentation variables to account for this. External cold does not affect the detectors because they are already cooled internally by LN. In the very conservatively chosen peak section **316**, the ratio of rates were  $R_{cold}/R_{warm} = (0.0065/s)/(0.0042/s) = 1.54$ . From measuring and comparing warm and cold singles rates in this same peak section **316** (a warm one is **MA**) the cold/hot ratio of singles rates was 1.07, and the cold/hot ratio of singles peak/Compton ratios was 1.03. Therefore, my method detects a gamma scattering property as a function of temperature that was not at all expressed in my singles spectrum. This experiment was repeated with similar results. An enhanced and spectrally narrowed Rayleigh scattering interaction is expected at lower temperatures due to less motion of the internal scattering centers. We take these scattering centers to be the chemical bond.

Towards determining the nature of the scattering site, the unquantum gamma-ray splitting technique shows that magnetism and temperature easily affect it. The method of this disclosure provides a unique sensitive probe to study short wavelength matter-wave fields under various applied physical conditions. It is a way to study bond structures.



The experimental data of Fig. **19** is to compare the unquantum effect of gamma-rays from two chemical states of Cd109: metallic and crystalline. The Cd109 was in a copper collimator with a 2 mm aluminum filter directing gamma-rays toward a 0.3 inch thick 2.2 inch diameter semiconductor grade germanium disk scatterer, taped onto the face of a 2 inch NaI(Tl) detector on channel 1. A second similar detector on channel 2 was placed away from direct rays of the source so that it only received gamma scattered from the germanium. The geometry of these components was similar to that shown in Fig. **17**. The source to scatter distance was 2 inches in the two tests.

The circuitry and the method of using the LT344 DSO was the same as described for Fig. 4.

In test of May 2  $\Delta t$  coincidence plot Fig 19 NB used a 30  $\mu\text{Ci}$  salt form of Cd109. Background was subtracted for these tests.  $R_e/R_c = (34.5 \times 10^{-6}/\text{s}) / (874 \times 10^{-9}/\text{s}) = 39.5$ .

In test of May 1  $\Delta t$  coincidence plot Fig. 19 NC used a 29  $\mu\text{Ci}$  metallic form of Cd109. The singles rates of the first detector were nearly the same at  $R_1$  23/sec and 24/s.  $R_e/R_c = (5.4\text{E}-6) / (760\text{E}-9/\text{s}) = 7$ .

The 5 fold greater unquantum effect of plot NB is attributed to the salt state of matter of the Cd109.

Fig. 20 now compares conventional gamma spectroscopy of these two states of Cd109, with an NaI(Tl) detector. Spectrum OA is from the salt Cd109 and spectrum OB is from the metal Cd109. The only difference is in Compton sections 336 and 334, being about 20%. It is unlikely that this difference can account for the much more dramatic change seen in the unquantum effect. Evidently photon violation spectroscopy can detect a wave-property of gamma-rays that is not detectable with normal gamma-ray spectroscopy.

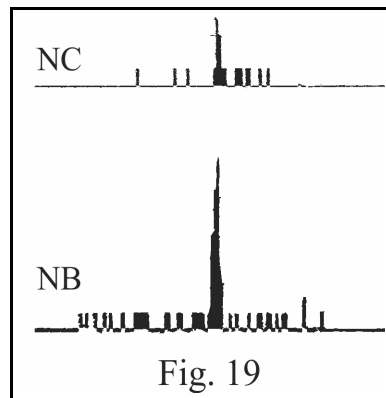


Fig. 19

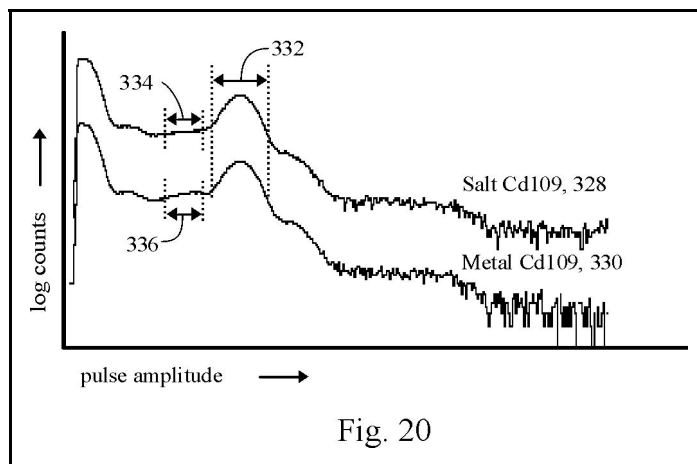


Fig. 20

## UNTESTED OBVIOUS APPLICATIONS

A sophisticated unquantum integrated circuit embodiment may be contemplated. To decrease experiment time, an array of detectors gated in coincidence from a central element of the array would avoid multiple positioning of a single channel-2 detector, such as 232 of Fig. 12. Diffraction crystallography algorithms may be employed to process the information to create images of atomic bonds. Such a diffractogram will have the advantage of creating images of flexible and stiff components of charge-wave microstructure using the window technique used for Fig. 15. Many modes of operation await future refinement. It is in these future refinements and experiments that the method of this invention has its most important utility.

## REMOVAL OF ARTIFACT

No doubt skeptics will say there must be some artifact at play. In search of artifact I have performed hundreds of tests: different geometries, experimental strategies, different detector types and sizes, different electronic components and arrangements, different isotopes, shielded background, tested effect of background, filtered cosmic ray pulses, tested for misshaped pulses, tested for pulse amplitude drift over time, tested for satellite PMT pulses, tested effects of a higher frequency contamination (Cd113m), eliminated lead fluorescence, tested with different shield and aperture metals at the source. I monitor every pulse counted in coincidence for uniform shape, and subtract background. Most importantly I have understood how to modulate the unquantum effect with conditions of the scatterer, source chemistry, and source distance while holding everything else constant. Also, in tests with noise and wide SCA settings I found that lowering noise and narrowing the SCA window improved the unquantum effect. Noise is not the source of my data.

Physicists have often challenged me with the idea that I have discovered something different

from what I say it is. Most often they think I discovered a new form of stimulated emission from the source that would shoot multiple simultaneously directed photons. The experiments above clearly do not fit this model, but I will address this issue directly. A simple calculation in Mossbauer theory shows the elements I have used at room temperature cannot undergo stimulated emission, but an experimental way to eliminate this possible cause is more convincing. In Fig. 10 there is a peak in plot **HB** at position **194**, I call the 2x peak, that requires three detections in coincidence: two events make that peak, plus one in the channel 1 detector. That peak **194** had 0.0013/s in just one bin. There is more than one bin at this 2x position. The spread is due to Compton down-shifting and summing with the coincident Cd109 x-ray. Let's conservatively take 5 bins to get  $5 \times 0.0013 = 0.0065/s$  detected in triple coincidence. In the ungated spectrum **HA** of data taken with the channel 2 HPGe detector in the same experimental arrangement, the rate in the single 88 keV bin was  $R_2 = 3/s$ . These detectors only have about 10% efficiency. So to calculate what was emitted, when we detect two at a time in the channel 2 detector we need to account for this efficiency two times. Therefore the detector is only able to detect two at a time at 1% efficiency, of what was emitted.  $(3 \text{ per sec})/100 = .03/s$  would need to be emitted three at a time aimed toward the channel 2 detector. That makes the ratio (detected/predicted) =  $0.0065/0.03$ . This means one in every 4.6 emissions would be emitted in triplicate in the same direction. In triplicate, because it was also detected with the channel 1 detector. The efficiency of the channel 1 detector was not accounted for, making this  $1/4.6$  a very conservatively calculated large fraction. So nearly every fictitious photon aimed at the detector would need to be emitted in a triple coincidence conspiracy to make what we see in Fig. 10. Experiments by others showing that it is extremely difficult to trigger a gamma emission, plus my above calculation eliminates any kind of stimulated emission theory.

The combination of unquantum effects displayed here and consistency among effects leave no room for doubt. There is no instrumentation or physical artifact at play to cause this unquantum effect, and I have found it useful in material science

investigation. There is no reason to think the unquantum effect is a special case for the two different isotopes I have described here. I have also seen success with Na22 and Am241. I expect other isotopes and sources will be discovered. Physicists can now test for themselves to find gamma-rays are not photons, and energy is not quantized.

## REFERENCES

NIELS BOHR, *Atomic Physics and Human Knowledge*, 1958, pgs. 50-51, John Wiley and Sons Inc, New York.

WERNER HEISENBERG, *The Physical Principles of the Quantum Theory*, 1930, pg, 39, Dover Publications Inc.

LOUIS DE BROGLIE, *An Introduction to the Study of Wave Mechanics*, 1930, pgs. 142-143 and 1-5, E. P. Dutton and Company Inc, New York.

M. P. GIVENS, "An experimental study of the quantum nature of x-rays," *Philosophical Magazine*, 1946, pgs. 335-346, vol. 37.

ERIC BRANNEN and H. I. S. FERGUSON, "The question of correlation between photons in coherent light rays," *Nature*, 1956, pages 481-482, vol. 4531.

JOHN F. CLAUSER, "Experimental distinction between the quantum and classical field theoretic predictions for the photoelectric effect," *Physical Review D*, 1974, pgs. 853-860, vol. 9.

JOHN F. CLAUSER, "Early history of Bell's theorem,"

*Coherence and Quantum Optics*  
VIII BIGELOW editor, 2003, pgs.  
19-43, Kluwer  
Academic/Plenum Publishers.

P. GRANGIER, G. ROGER, A.  
ASPECT, "A new light on single  
photon interferences," *Annals of  
the New York Academy of  
Sciences*, 1986, pgs. 98-107, vol.  
480, New York.

ARTHUR L. ROBINSON,  
"Demonstrating single photon  
interference," *Science*, 1986,  
pgs. 671-672, vol. 231.

THOMAS S. KUHN, *Black-  
Body Theory and the Quantum  
Discontinuity 1894-1912*, 1978,  
pgs. 235-264, Oxford University  
Press, New York.

MAX PLANCK, "Eine neue  
Strahlungshypothese" (1911),  
*Physikalische Abhandlungen  
und Vorträge*, 1958, pgs. 249-  
259, vol. 2, [see eq. 14] Carl  
Schütte & Co, Berlin.

MAX PLANCK, *The theory of  
heat radiation*, 1913, p. 153,  
Dover, New York.

P. DEBYE, A. SOMMERFELD,  
"Theorie des lichtelektrischen  
effektes vom standpunkt des  
wirkungsquantums," *Annalen  
Der Physik*, 1913, pgs. 872-930,  
vol. 41, Leipzig.

ARTHUR H. COMPTON,  
SAMUEL K. ALLISON, *X-Rays  
in Theory and Experiment*, 1935,  
p. 47 and pgs. 232-233, second  
edition, Macmillan and Co,  
London.

ROBERT ANDREWS  
MILLIKAN, *Electrons (+ and  
-), Protons, Photons,  
Neutrons, Mesotrons, and  
Cosmic Rays*, 1947, p. 253,  
revised edition, University of  
Chicago Press, Chicago.

H. A. LORENTZ, Die  
hypothese der lichtquantin,  
*Physik. Zeitschrift*, 1910, pgs.  
349-359, vol. 11.

G. P. THOMSON, *The Wave  
Mechanics of Free Electrons*,  
1930, p. 127, McGraw-Hill,  
New York.

ALBERT EINSTEIN, "On a heuristic  
point of view concerning the  
production and transformation of  
light" (title translated), *Annalen der  
Physik*, 1905, pgs. 132-148, vol.  
17.

ARNOLD SOMMERFELD,  
*Wave-Mechanics*, 1930, p. 178,  
Methuen & Co, London.

E. SCHRÖDINGER,  
"Quantization as a problem of  
proper values" (title translated),  
*Annalen der Physik*, 1926, vol.  
79, translated in *Collected  
Papers on Wave Mechanics*,  
1978, Chelsea Publishing  
Company, New York.

MAX BORN, *Atomic Physics*,  
1935, p. 89, fifth edition,  
Hafner Publishing Company,  
New York.

ROBERT S. SHANKLAND,  
"An apparent failure of the  
photon theory of scattering,"  
*Physical Review*, 1936, pgs. 8-  
13, vol. 49.

A. Bernstein, A. K. Mann,  
“Summary of recent  
measurements of the Compton  
effect,” *American Journal of  
Physics*, 1956, pgs. 445-450,  
vol. 24.

W. BOTHE, H. GEIGER, “Über  
das Wasen des Comptoneffekts,”  
*Zeitschrift für Physik*, 1925, pgs.  
639-663, vol. 32.

ARTHUR H. COMPTON,  
ALFRED W SIMON, “Directed  
quanta of scattered x-rays,”  
*Physical Review*, 1925, pgs. 289-  
299, vol. 26.

ARTHUR H. COMPTON,  
“What things are made of,”  
*Scientific American*, Feb. 1929,  
pages 110-113.

DAVID HALLIDAY, ROBERT  
RESNICK, *Fundamentals of  
Physics*, 1986, pgs. 842-843,  
second edition, John Wiley and  
Sons, New York.

ERNEST O LAWRENCE, J. W.  
BEAMS, “The element of time  
in the photoelectric effect,”  
*Physical Review*, 1928, pgs. 478-  
485, vol. 32.

CARL A. KOCHER, EUGENE  
D. COMMINS, “Polarization  
correlation of photons emitted in  
an atomic cascade,” *Physical  
Review Letters*, 1967, pgs. 575-  
577, vol. 18.

C. M. DAVISSON, “Interaction  
of  $\gamma$ -radiation with matter,”

*Alpha Beta and Gamma-ray  
Spectroscopy* KAI SIEGBAHN  
editor, 1966, p. 37, vol. 1,  
North-Holland Publishing,  
Amsterdam.

*Photomultiplier tubes  
principles and applications*,  
1994, pgs. 2-8, Philips  
Photonics, Brive, France.

RICHARD P. FEYNMAN,  
*QED*, 1985, p. 15, Princeton  
University Press, Princeton.

GLENN F. KNOLL, *Radiation  
Detection and Measurement*,  
1979, pgs. 690-691, John Wiley  
& Sons, New York.

J. J. KRAUSHAAR et al,  
“Comparison of the values of  
the disintegration constant of  
 $Be^7$  in Be, BeO, and BeF<sub>2</sub>,”  
*Physical Review*, 1953, pgs.  
610-614, vol. 90.

ARTHUR H. COMPTON,  
OSWELD ROGNLEY, The  
nature of the ultimate magnetic  
particle, *Science*, Oct. 26, 1917,  
pgs. 415-416, vol. XLVI.